Quantitation of Halogenated Anisoles in Wine via SPME – GC/MS

by

John A. Milo

Submitted in Partial Fulfillment of the Requirement

for the Degree of

Master of Science

in the

Chemistry Program

YOUNSTOWN STATE UNIVERSITY

December, 2008

Quantitation of Halogenated Anisoles in Wine via SPME – GC/MS

John A. Milo

I hereby release this thesis to the public. I understand that this thesis will be made available from the OhioLINK ETD Center and the Maag Library Circulation Desk for public access. I also authorize the University or other individuals to make copies of this thesis as needed for scholarly research.

Signature:

John A. Milo Date

Approvals:

Dr. Brian D. Leskiw Date
Thesis Advisor

Dr. Roland Riesen Date
Committee Member

Dr. Larry Curtin Date
Committee Member

Dr. Peter J. Kasvinsky Date
Dean of School of Graduate Studies and Research

Abstract

This research study involves the development and optimization of solid-phase microextraction (SPME) coupled with gas chromatography-mass spectrometry (GC-MS) for the analysis of halogenated anisoles present in wines at ultra-trace amounts. The presence of these compounds in wines unfortunately affects the aroma, ruins the overall taste, and accounts for huge monetary losses in the wine industry every year. The work described herein focuses on the quantitation of these undesirable compounds at levels below olfactory threshold limits and the development and validation of the extraction procedure method associated with SPME. Multiple commercial wine samples, contaminated with these unwanted compounds, were analyzed where the actual amount of halogenated anisoles was determined.

Acknowledgements

First and foremost, I would like to thank my family for all their love and support through this process. Special recognition goes to my parents, Kerry and Elizabeth. Without the sacrifices they have made throughout my life, I could not have achieved as much as I have. The compassion they posses has helped me complete this venture along with many other goals.

I also wish to thank my advisor Dr. Brian D. Leskiw for helping me with any type of issue I had, whether research related or not, he always found the time to help in any way he could. His encouragement during graduate school was invaluable, and I am thankful to have had him as an advisor. Special thanks goes to Dr. Roland Riesen. Without his valuable direction in passing along his knowledge whenever I hit a barrier in research would have made this process considerably more difficult. Thanks goes to Ray Hoff for providing technical support for the instruments and providing hands on experience to learn the functions of the equipment.

I wish to thank Dr. Larry Curtin for choosing to be on my committee and for his positive suggestions on my research and thesis.

I would also like to thank my colleagues in the YSU Chemistry Department who have lent a hand whenever I was in need. Calvin Austin, Jordan Lerach, and Jerry Hunter all have made my stay at YSU more pleasurable and have given me help through many difficult processes. Thanks goes to the Youngstown State University Department of Chemistry and the Office of Graduate Studies for support on this research project.

Table of Contents **Page**

List of Figures **Page**

List of Tables **Page**

List of Equations **Page**

List of Abbreviations

A_S	Peak symmetry
DC	Direct-current
DVB/CAR/PDMS	Divinylbenzene/carboxen/polydimethylsiloxane
EI	Electron impact
EtOH	Ethanol
GC	Gas chromatography
GC/MS	Gas chromatography/mass spectrometry
k'	Capacity factor
LOD	Limit of Detection
LOQ	Limit of Quantitation
MS	Mass spectrometry
m/z	*Mass-to-charge* ratio
N	Number of theoretical plates (symmetrical peak)
N^*	Number of theoretical plates (asymmetrical peak)
NaCl	Sodium Chloride
PA	Polyacrylate
PCA	Pentachloroanisole
R^2	Coefficient of determination
RF	Radio frequency
R_S	Resolution
RSD	Relative standard deviation
SIM	Selected ion monitoring

SIS	Selected ion storage
S/N	Signal to noise
sV/vV	Sample volume/vial volume
SWS#1	Synthetic working solution one
SWS#2	Synthetic working solution two
TBA	2,4,6-Tribromoanisole
TCA	2,4,6-Trichloranisole
TCA-d_5	2,4,6-Trichloroanisole-d_5
TCT	2,3,6-Trichlorotoluene
TeCA	2,3,4,6-Tetrachloroanisole
TIC	Total ion count
SPME	Solid-phase microextraction

Chapter I

Literature Review

A. Wine Analysis

Many chemical components make up the composition of a wine. These compounds are organized into several organic classes which include organic acids, polyol's, simple alcohols, fatty acids, esters, aldehydes, ketones, and carbohydrates [1]. Many of these compounds are volatile and affect the aroma, which in turn, alters the taste of the wine. Most volatile compounds in wines are present in trace amounts, where the olfactory perception of the volatile compounds depends on both their type and concentration.

Wine aromas are very complex, which makes them difficult to study. Numerous factors contribute to its aroma. For example, grape variety plays a distinct role in the quality and regional character of a wine as soil conditions and climate vary. Another factor contributing to the quality of wine is the amount of oxidation and hydrolysis prior to fermentation, as these reactions have been found to influence the development of the aroma. During the fermentation process, microorganisms dictate the amount of alcohol and the malolactic conversion. Malolactic conversion occurs when lactic acid bacteria convert the lactic acid present in the must (or wine) into malic acid, giving the wine a rounder and fuller flavor. In the aging process following fermentation, chemical or enzymatic reactions occur which subsequently develop the color, aroma, and flavor of the wine.

B. Targeted Components Effecting Aroma in Wines

During the storage and aging of a wine, organoleptic defects can occur resulting in a musty, moldy, "wet cardboard" aroma termed “cork taint.” Such organoleptic defects give a combined annual loss of $10 US billion to the industry [2]. Haloanisoles have been identified as a main contributor to several unpleasant smells in wines and originate from reactions involving the natural cork oak, *Quercus Suber* [3]. Haloanisoles penetrate into the wine from an infected cork, to give the liquid an “off aroma” and compromised taste.

The main haloanisoles are 2,4,6-trichloroanisole (TCA), 2,3,4,6-tetrachloroanisole (TeCA), pentachloroanisole (PCA), and 2,4,6-tribromoansiole (TBA). These four compounds have an olfactory detection threshold in the low ng L^{-1} range making them very pungent in ultra-trace amounts. These compounds form (as illustrated in Figure 1.1) following halogenation reactions of phenols, a common byproduct of wood. This halogenation is performed by microbiotics, hypochlorite, previous pesticides, or disinfecting cleansers on the cork before bottling the wine. Finally, *O*-methylation occurs to change the halogenated phenols to haloanisoles. This happens by a reaction that molds, fungi from the aspergillas family [4], and yeasts produce in the lenticels of the cork. Once these compounds are formed, simple diffusion from the cork occurs and the haloanisoles penetrate into the wine and severely alter the product.

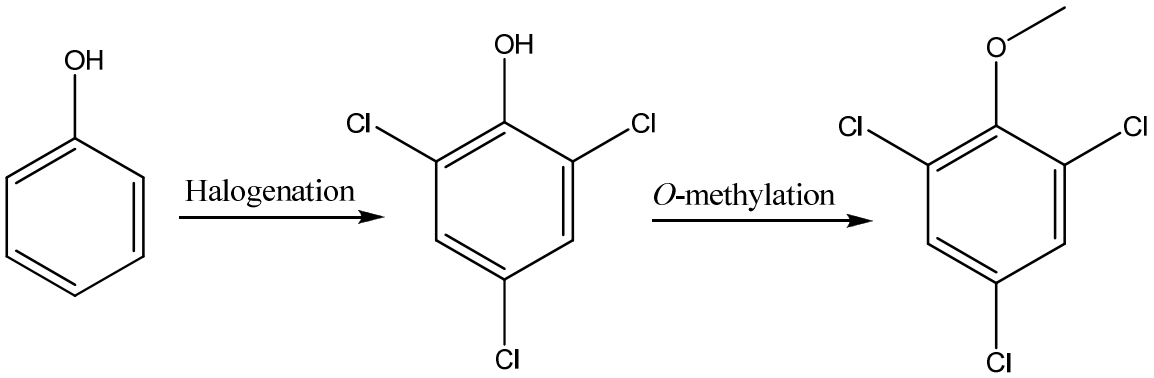

Figure 1.1: Reaction scheme involving the formation of TCA from phenols.

C. Extraction Methods

Before the analysis of any compound can be performed, the analyte must be removed from the original solution and relocated to a targeted site, for instance, the injector of the gas chromatograph. This method is called extraction, and numerous methods exist. The more traditional methods include liquid-liquid extraction, distillation, and solid-liquid extraction. These techniques extract the targeted compounds with harsh organic solvents, require a large sample size, and are prone to the loss of analytes [5]. In addition, these techniques are quite time consuming, and consequently are not commonly used. The more modern and selective extraction techniques are increasingly common and include supercritical fluid extraction (SFE) [6], purge and trap [7], solid-phase extraction (SPE) [8], stir bar sorbtive extraction (SBSE) [9-10], and solid-phase microextraction (SPME) [4,5,11-14].

Solid phase microextraction is an extraction technique which allows for both the extraction and concentration of the analyte to be done simultaneously on volatile compounds. This technique is solvent free, requires no pre-concentrating steps of the analytes, and drastically reduces sample preparation time [11]. The first SPME apparatus

was developed by Arthur and Pawliszyn in 1990, and was a technique used for preconcentrating water pollutants before analysis [14]. This extraction technique has since been optimized for other targeted volatile compounds in other applications. SPME is frequently coupled with gas chromatography mass spectrometry (GC-MS).

SPME inserts a porous needle filament into the sample headspace and adsorption of the analyte occurs in the gaseous phase until the filament reaches a point of saturation. Upon equilibrium, the initial analyte concentration can be calculated. According to Lizarraga [4] the targeted compounds will evenly distributed between the three phases; sample, fiber, and headspace:

$$C_0 V_s = C_f V_f + C_h V_h + C_s V_s \qquad \text{Equation 1.1}$$

where C_0 is the initial concentration of analyte present in sample, V_s is the volume of the sample solution, C_f, C_h, and C_s are the concentrations at equilibrium of the analytes in the fiber, headspace, and the sample respectively. V_f, V_h, and V_s are the volumes of the fiber, headspace, and sample. From this, the ratio of the concentrations of each component in the three different phases can be expressed as equilibrium constants:

$$K_{fh} = \frac{C_f}{C_h},\ K_{hs} = \frac{C_h}{C_s}, \text{ and } K_{fs} = \frac{C_f}{C_s}.$$

These constants describe the equilibrium between the fiber and headspace, headspace and sample, and the fiber and sample. Ideally, the amount of the analyte adsorbed by the fiber at equilibrium is proportional to the concentration of the analytes in the sample and can be described by the following equation:

$$n = \frac{K_{fs} V_f C_0 V_s}{K_{fs} V_f + K_{hs} V_h + V_s} \qquad \text{Equation 1.2}$$

where n is the mass of analyte adsorbed by the fiber, V_s is the sample volume. The sample volume is typically much larger than the equilibrium constants $K_{fs} V_f$ and $K_{hs} V_h$, therefore minimizing their role in Equation 1.2. In addition, the quantity of analyte adsorbed by the fiber is not dependent on the sample volume, but relative to K_{fs} and V_f, with Equation 1.2 simplifying to:

$$n = K_{fs} V_f C_0$$

There are multiple types of SPME fibers available. Some SPME fibers have a liquid coating, such as polydimethylsiloxane (PDMS) and polyacrylate (PA), and extraction occurs with these fibers when the targeted analytes absorb directly into the fiber coating. Other fibers consist of a porous solid, for instance PDMS-DVB (divinylbenzene) and Carbowax/DVB, where the analytes are adsorbed directly onto the fiber [15]. The DVB/CAR/PDMS fiber has been shown to have the best extraction efficiency for haloanisoles at a high extraction temperature [13-14], while the PA fiber is best for phenols, due to the polarity of the molecules [13]. The properties of compounds of interest must be closely examined to determine what fiber type will yield the best extraction efficiency.

Several factors control the efficiency of the SPME fiber. These factors should be evaluated and optimized in order to increase analyte adsorption. The key factors include sample agitation, sample volume versus sample size, salt addition to the sample prior to extraction, extraction time, and extraction temperature.

Sample agitation during extraction influences the transfer of analytes from the liquid phase into the gas phase, which allows for a quicker adsorption time. Sample volume versus sample size must be analyzed to determine the correct ratio for each analyte to indicate the best relationship. Another parameter observed to have a noticeable affect is salt addition. As the ionic strength of the matrix increases, the solubility of the analyte decreases thus increasing the sensitivity as the analytes more readily partition into the gas phase. The "salting-out" effect is dependant on each compound [13], and the degree of saturation must be examined for every analyte. Usually, a variety of analytes are studied simultaneously, where a compromise must be made for the best ratio.

Extraction temperature also plays a vital role in the extraction process. The temperature affects the partition coefficient of the analytes between the sample matrices and the fiber coating at a constant rate [14]. By increasing the extraction temperature, the mass transfer of the analytes to the fiber will increase, thus decreasing the time taken for the SPME fiber to reach equilibrium. Another parameter to evaluate is extraction time, where the exposure time required to achieve the best extraction efficiency is dependent on the actual compounds. Certain analytes may reach equilibrium quickly, while others may take much longer. Consequently, an appropriate extraction time must be determined to yield the desired sensitivity for all compounds of interest.

D. Quantitative Analytical Methods

A main problem with SPME and is matrix interferences. The standard addition technique is often used to overcome matrix effects where a fixed amount of desired analyte is added to the sample. That sample is analyzed and the difference between the

amount added and total measured analyte concentration is the initial concentration present in the sample. This process is done by increasing the concentration of the analyte multiple times linearly and establishing a standard addition curve. A standard addition curve must be performed every time a sample is run, making the process long and tedious.

Another technique which overcomes these interferences is the internal standard method. This method adds a reference standard to the sample, and the response of the solute of interest is compared to the reference as a function of analyte concentration to the standard as shown in the following equation:

$$\frac{c_r}{c_{st}} = \frac{a_r}{a_{st}}\alpha_r \qquad \text{Equation 1.3}$$

In Equation 1.3, c_r is the concentration of the analyte, c_{st} is the concentration of the internal standard, a_r is the area of the peak for the analyte, and a_{st} is the area of the peak for the internal standard. The response factor, α_r, can be calculated by rearranging Equation 1.3 as:

$$\alpha_r = \frac{c_r a_{st}}{c_{st} a_r}$$

The reference standard must share the same chemical properties as the desired solute, therefore during the experimental procedure, no loss of the internal standard will occur.

E. Chromatography

Chromatography is a separation technique that physically partitions the components to be separated between the mobile phase and stationary phase. In

chromatographic methods, separation occurs following the distribution of the analyte in the sample between the two phases. The mobile phase in chromatography is either a gas or a liquid, and the stationary phase is either a viscous liquid chemically bonded to the inside of the capillary tube, or a solid packed on the inner surface of the column. The mobile phase is often driven through the column at a constant rate. The amount of interactions between the analyte with the stationary and mobile phases determines the degree of separation.

In gas chromatography (GC), open tubular columns are primarily used where the stationary phase is coated on the inside walls of the capillary. The mobile phase is a highly pure inert gas, usually helium or nitrogen, and is driven through the column at a constant rate. Each analyte has a unique partitioning in and out of the stationary and mobile phases. This partitioning is based upon the molecular weight, vapor pressure, polarity, and intermolecular forces of the molecules involved.

GC is an example of elution chromatography where the mobile phase is added at a constant rate after the application of the analytes, *via* injection. The analytes elute through the entire length of the column and are detected as function of time. The partitioning in and out of the stationary and mobile phases can be determined by the following equation:

$$K_d = \frac{C_s}{C_m} \qquad \text{Equation 1.4}$$

where K_d is the partition coefficient, C_s is the molar concentration of the analyte in the stationary phase, and C_m is the molar concentration of the analyte in the mobile phase. The partition coefficient ratio can be used to determine how fast an analyte will take to

move through the column. Greater separation between solutes can be achieved when K_d is large.

The time that the sample interacts in the stationary phase is relative to the time it exists in the mobile phase. Each peak in a chromatogram has a capacity factor, k', which is defined as:

$$k' = \frac{t_r - t_m}{t_m} \qquad \text{Equation 1.5}$$

where t_r is the retention time taken for an analyte to elute, and t_m is the dead time or the time required for only the mobile phase to elute. A large k' indicates more interactions between the analyte and stationary phase giving a longer elution time. A small k' corresponds to less interaction between the analyte and the stationary phase, indicating a shorter elution time.

The linear velocity is defined as the rate of change of the position of the mobile phase. The mobile-phase velocity, which is the carrier gas, can be determined by:

$$u = \frac{l}{t_m} \qquad \text{Equation 1.6}$$

where u is the linear velocity of the carrying gas in cm/min and l is the length of the column. The dead time reference point is established from the linear velocity.

The volume of the mobile phase required to elute a particular solute from the column can be calculated from:

$$V_r = t_r \cdot u_v \qquad \text{Equation 1.7}$$

where V_r is the retention volume and u_v is the volume flow rate (volume per unit time) of the mobile phase. Retention time, t_r, is the time required to elute a solute, at its

highest concentration, through the column. Retention time is related to retention volume by the following equation:

$$t_r = \frac{V_r}{F} \qquad \text{Equation 1.8}$$

with the flow, F, described by:

$$F = \frac{r_c{}^2 l}{t_m} \qquad \text{Equation 1.9}$$

where the radius of the column is r_c, the column length, l (in centimeters), and the dead time, t_m, is expressed in minutes.

Martin and Synge suggested that a chromatographic column consists of a series of thin, neighboring sections called "theoretical plates." These plates permit a partition of the solute between the mobile and stationary phases. This process is viewed as a stepwise transfer from one plate to the next. The thickness, or height of the theoretical plate, H, can be calculated by dividing the length of the column by the total number of theoretical plates, N:

$$H = \frac{l}{N} \qquad \text{Equation 1.10}$$

The number of theoretical plates can be calculated for peaks that exhibit a Gaussian shape:

$$N = 16\left(\frac{t_r}{W_b}\right)^2 \qquad \text{Equation 1.11}$$

where W_b is the width of the peak at the base. For peaks that have a non-Gaussian shape peak with asymmetrical edges, a modified form of Equation 1.11 is used to compensate for the irregular peak shape:

$$N^* = 5.54\left(\frac{t_r}{W_{1/2}}\right)^2$$

where $W_{1/2}$ is the width of the peak at half of the peak height, illustrated in Figure 1.2. Measuring the peak at half of the height minimizes the effect of the irregular shape (fronting or tailing). The more "theoretical plates" that exist within a column, the better separation capabilities it will have.

Peak resolution describes how well two adjacent peaks are separated in a chromatogram, as illustrated in Figure 1.2. The resolution factor, R_s, is the distance between two peaks divided by the average extrapolated base width of the peaks:

$$R_s = \frac{2\left(t_{r,B} - t_{r,A}\right)}{W_A + W_B} \qquad \text{Equation 1.12}$$

A resolution factor below 1, indicates that the adjacent peaks overlap one another, while R_s = 1 designates that the peaks are adequately resolved for quantitation but do not have baseline resolution. Baseline resolution is achieved when the signal returns back to the background level before for the start of any subsequent peak. This occurs when the R_s > 1, and is needed for good separation and the determination of analyte peak areas.

To measure peak symmetry a vertical line is drawn from the apex of the peak to the baseline. The peak width before and after the apex line at 10% of the total peak

height is measured and the peak symmetry is calculated described by the following equation:

$$A_s = \frac{b}{a} \qquad \text{Equation 1.13}$$

where b is the peak width after the apex, and a is the width before the line. A value of $A_s < 1$ indicates a fronting peak, $A_s > 1$ is a tailing peak, and $A_s = 1$ is a mathematically symmetrical peak.

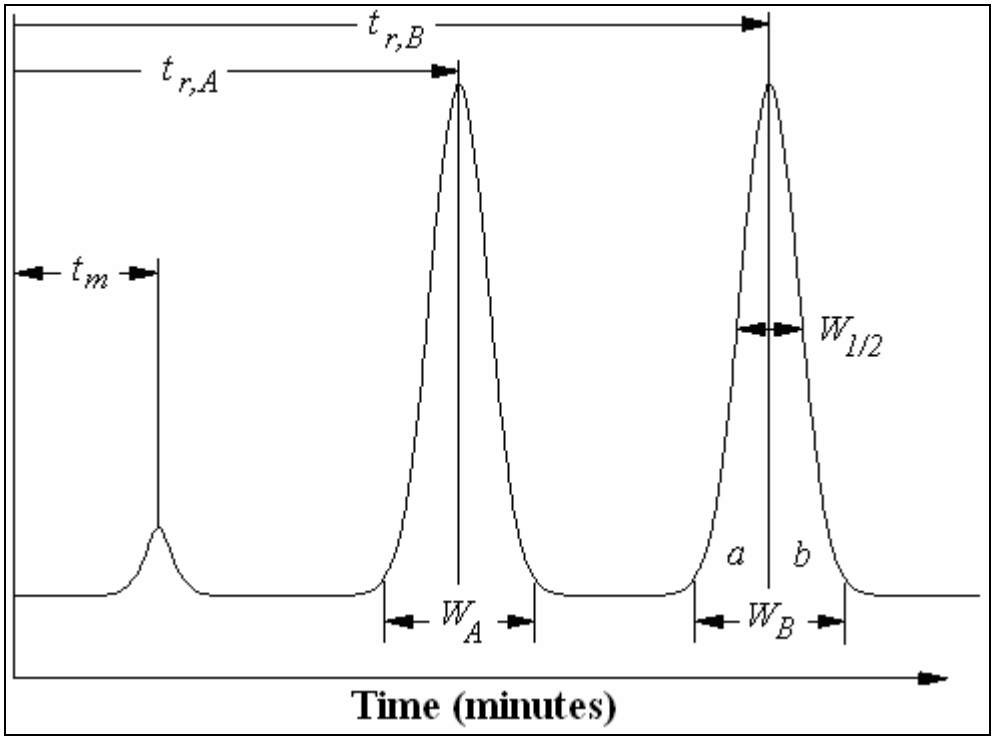

Figure 1.2: Measurements used to calculate the chromatography of a column.

F. Mass Spectrometry

Mass spectrometry (MS) is an analytical technique which determines the chemical composition of a molecule from its *mass-to-charge ratio* (*m/z*). The charge and degree of ionization the molecule undergoes is determined by the energy transfer during the

ionization process [18]. Once the molecule is an ion, mass analysis can identify its *m/z* ratio, and a mass spectrum over a particular range can be created. The mass spectrum will give the intensities of the analyte ions, which can then be used to determine the concentration of the desired analytes if an appropriate calibration is conducted.

Ionization techniques vary and the type employed depends on the stability of the samples of interest. The ionization techniques can be categorized in two main groups: harsh versus soft. Harsh ionization gives the molecule more energy than required for it to become ionized and often results in molecule fragmentation. Electron impact (EI) is the most commonly used type:

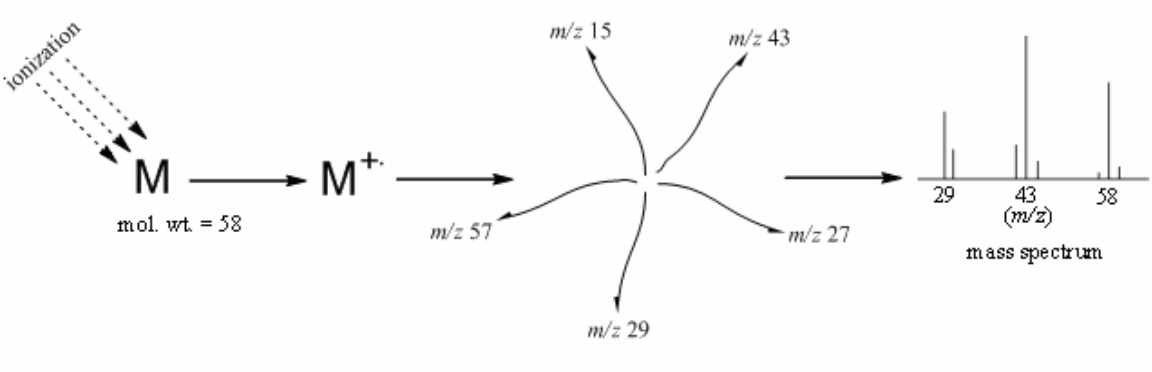

Figure 1.3: General scheme of electron impact ionization of a gaseous molecule [19].

where initially the sample M, which is a neutral gaseous molecule, is bombarded with electrons and ionized. The excess energy is dispelled through fragmentation of weaker chemical bonds, where this cleavage yields the production of the fragmented ions whose masses all sum to the mass of the parent molecule [19].

A "soft" ionization technique typically involves the ionization of an analyte that is fragile or nonvolatile. Biopolymers, proteins, sugars, and biological samples often

require this type of ionization. This ionization is called "soft" because there is limited fragmentation of the original molecule. Figure 1.4 shows how this nondestructive process takes place since the original molecule is present with the addition of single and/or multiple protons. Protonation occurs due to the charged reagent gas donating a proton/s (H^+) to the analyte (M).

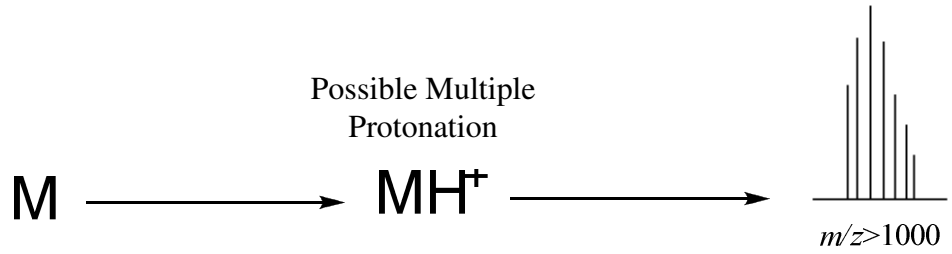

Figure 1.4: General scheme of chemical ionization on a nonvolatile molecule [19].

Once the ions are formed in the mass spectrometer, a mass analyzer separates them according to their *m/z* ratio. Many types of mass analyzers exist, including; time of flight, magnetic sectors, ion cyclotron resonance, quadrupole, and quadrupole ion trap. A quadrupole ion trap mass analyzer was used in this work.

A quadrupole consists of four parallel rods which filter the ions by a combination of direct-current (DC) and radio frequency (RF) fields. These two electric fields oscillate the charge which makes the ions flow toward and away from the rods in a wavelike fashion. Ions which do not posses the correct *m/z* ratio will oscillate at a too large or small of a trajectory causing them to go off axis and never make it to the detector. As ions leave the source and travel the length of the instrument, only ions that match a

particular *m/z* will reach the detector and be detected. Ions not matching the particular *m/z* will have an off axis trajectory and not be detected.

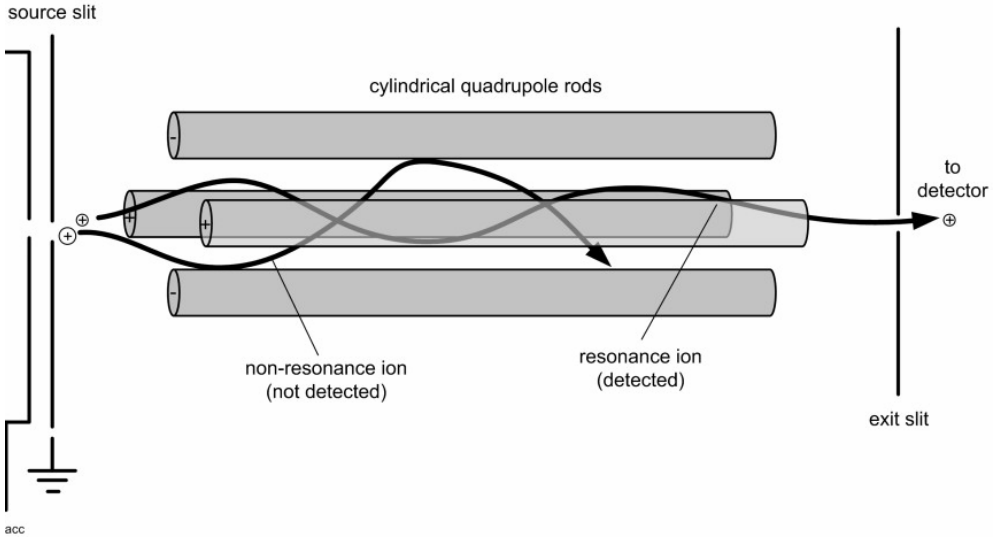

Figure 1.5: Schematic diagram of a quadrupole mass analyzer illustrating flight pattern of ions [20].

A quadruple ion trap is similar to a quadrupole mass analyzer by the use of oscillating DC and RF fields. In a quadrupole ion trap, however, the ions are trapped in a three-dimensional space whereas quadrupole mass analyzers use only two-dimensional confinement [19]. In the interior volume, the ions are trapped within the two endcaps and ring electrodes as seen in Figure 1.6:

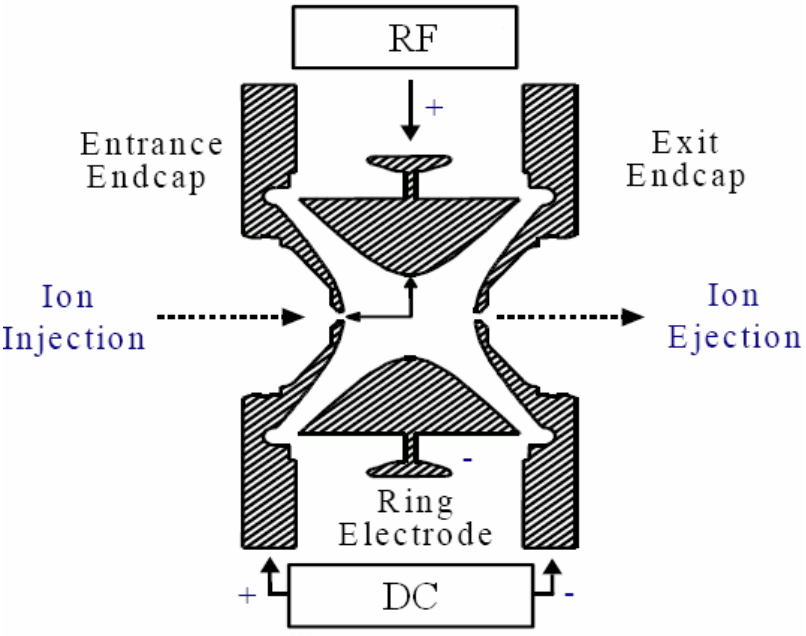

Figure 1.6: Schematic diagram of a quadrupole ion trap mass analyzer cross-section [21].

A quadruple ion trap is utilized in the work presented here where ions of a specific *m/z* are trapped and collected in three-dimensional space, ejected, and then analyzed.

G. Gas Chromatography Mass Spectrometry

The process of coupling gas chromatography to a mass spectrometer yields a complimentary relationship. The GC can effectively separate the analytes within a multianalyte sample which, in turn, greatly simplify the mass spectrometric analysis. This provides an opportunity to analyze multiple compounds within a potentially complex sample in a very simple manner. The use of GC/MS yields a powerful analytical tool which allows for the identification and quantitation of analytes.

Chapter II

Experimental

A. Chemicals and Reagents

All standards and reagents were obtained in the highest purities available. Listed below in table 2.1 are the chemicals with their CAS number, purity, and source.

Standard or Reagent	CAS number	Percent Purity	Source
Ethanol, Absolute	64-17-5	≥99.5	Acros Organics
Ethanol, Absolute	64-17-5	≥99.5	Sigma-Aldrich
Tartaric Acid	87-69-4	99+	Acros Organics
2,4,6-Trichloroanisole	87-40-1	99	Supelco
2,3,4,6-Tetrachloranisole	938-22-7	99	Ultra Scientific
2,4,6-Tribromoanisole	607-99-8	99	Sigma-Aldrich
Pentachloroanisole	1825-21-4	99	Chem Service Inc.
2,3,6-Trichlorotoluene	2077-46-5	96	Ultra Scientific
2,4,6-trichloroanisole-d_5	352439-08-8	Analytical Standard	Sigma-Aldrich
Sodium Chloride	7647-14-5	99.9	Fisher Scientific
Sodium Hydroxide	1310-73-2	95+	Fisher Scientific
Hydrochloric acid	7647-01-0	36.5-38	Pharmco-AAPER
Water, Milli-Q filtered	7732-18-5	-	In-house

Table 2.1: Chemical standards, CAS number, purity, and source.

B. Standard Solutions and Samples

Individual stock standards of each haloanisole, trichlorotoluene (TCT), and 2,4,6-trichloroanisole-d_5 (TCA-d_5) were first dissolved in ethanol at 100 mg/L, and then diluted to 100 µL/L for each analyte. The stock solutions of 100 µL/L were further diluted with a 4:1 Milli-Q water/99.5% ethanol solution to a concentration of 10 µL/L. Hydro-alcoholic solutions were used instead of strictly ethanol to minimize the altering of the

alcohol concentration during spiking of the samples. All solutions were stored in darkness at 4 ºC.

A synthetic model wine solution, which mimics the nature of wine, was prepared using 7.0 g/L tartaric acid in a hydro-alcoholic solution (12% (v/v) ethanol). The pH was adjusted to 3.4 using sodium hydroxide and reflects the fact that white wine is slightly more acidic than red wine.

Once the model wine solution was prepared, working solutions were made by diluting various amounts of the final standard solutions in either model wine or real wine [Carlo Rossi Reserve Cabernet Sauvignon (ethanol content 11.4% v/v), Carlo Rossi Reserve Chardonnay (ethanol content 12.1% v/v), or 1992 David Bynum Limited Edition Russian Valley River Pinot Noir (ethanol content 13.1% v/v)], which were absent of cork taint, 2,3,6-trichlorotoluene, and 2,4,6-trichloroanisole-d_5.

Commercial wines, which were believed to be contaminated with at least one of the four haloanisoles, were provided by Dr. Roland Riesen. These commercial wine samples were frozen until optimization research was completed and validated. The commercial wine samples were thawed and kept at 4 °C in the dark until analysis. Listed in Table 2.2 are the commercial wine samples with their measured ethanol content:

Sample	Wine	Ethanol Content (v/v)
1	2003 Turley California Zinfandel Juvenile	16.1%
2	2000 Cuvée Réservée Chateauneuf du Pape	15.1%
3	1999 E. Guigal Brune Et Blonde de Guigal	14.1%
4	1993 Clos des Papes Chateauneuf du Pape	13.9%
5	2000 Chateau Chaurin Grand Cru Classé St. Emilion	14.0%
6	1997 McCrea Syrah	14.1%
7	1988 Chateau Montelena Cabernet Sauvignon	13.9%
8	Las Tablas Estates Glenrose Vineyard (Syrah 35%, Mourvédre 29%, Grenache 26%, Counoise 10%)	15.3%
9	2003 Rosenblum Cellars Zinfandel Rockpile Road Vineyard	17.0%
10	105 Siduri Vanderkamp Pinot Noir	15.9%
11	Unknown #11	15.1%
12	105 Chasseur Sexton P.N.	16.0%
13	103 J.C. Cellars Frediani P.S.	17.3%
14	2000 Chateau Rocher Bellevue Caprice D'Angélique	13.4%

Table 2.2: Contaminated commercial wines for analysis.

C. Preparation of Commercial Wine Samples

Initially the alcohol percentage of the wine was measured to determine the correct concentration prior to dilution on an Ebuliometer supplied by Dujardin Salleron (made in France). Upon analysis, the wine sample was then diluted until the ethanol content was at 11.0% (±0.1%) and the final volume was 35 mL. 105 µL of the internal standard (TCA-d_5, concentration 10µL/L) was added to the mixture and immediately mixed. 10 mL was placed in clear 23 x 75 mm vials (MicroLiter Analytical Supplies, Inc.), with 1.0 g of NaCl, and immediately sealed with a metal LO seal, 20 mm w/tan PTFE with a white silicone septum (MicroLiter Analytical Supplies, Inc.).

D. Equipment

The SPME-GC/MS analysis was preformed on a Varian 3800 gas chromatograph equipped with a Combi Pal autosampler connected to a Varian Saturn 2000 quadrupole ion trap mass spectrometer. The software the system used was Varian MS workstation version 6.9.

E. Chromatographic Conditions

In the beginning of this research the carrier gas was BIP (built in purifier) helium supplied by Airgas (Great Lakes) at one mL/min, but as this gas became no longer available, 5.0 ultra high pure (UHP) grade helium from Praxair, Inc. (Danbury, CT) was employed instead. This UHP helium was filtered in this process:

i. Varian carrier gas filter (hydrocarbons and water)
ii. Varian gas purifier (hydrocarbons and water)
iii. Varian gas clean moisture filter
iv. Varian gas clean oxygen filter

The injector was fitted with a Merlin Microseal septum for 1079 injector 23 gauge with a Varian deactivated 1078/1079 glass insert, SPME, 0.8 mm ID. Injection was performed in splitless mode at an inlet temperature of 250˚C in the preliminary research and 270 ˚C after optimization for the VF-5ms capillary column. The SPME fiber selected was a 23-gauge, 50/30 µm, divinylbenzene/carboxen/polydimethylsiloxane (DVB/CAR/PDMS) assembly supplied by Supelco (Bellefonte, PA) and was conditioned according to the manufacturer's specifications. Separation of the compounds was achieved by a Varian FactorFour VF-5ms capillary column (30m × 0.25 mm I.D. × 0.25 µm film thickness).

F. Detection Conditions

The oven temperature was programmed as follows: initially at 50 ˚C for 2 minutes, then heated at 5 ˚C/min to 100 ˚C and kept for 1 minute. Next, heated to 170 ˚C at 3 ˚C/min; and finally raised to 250 ˚C at 15 ˚C/min and maintained for 3 min. The manifold, trap, and transfer line were kept at 40 ˚C, 150 ˚C and 275 ˚C, respectively. Mass spectra were obtained using electron impact ionization (70eV), and the instrument was operated in SIS mode for the selected ions of each analyte.

Chapter III

Method Development

For the optimum analysis of a particular sample, the development of a suitable analytical method is required. The techniques of the method must compliment the samples studied, where various parameters of the technique must be evaluated. When SPME, coupled with GC/MS, is used to investigate volatile compounds, several factors control the overall efficiency of extraction, and include the fiber type, extraction time, extraction temperature, and the sample matrix. The sample matrix, especially in wines, is predominantly different from sample to sample, which can cause a variation of extraction efficiency. This potential variation brings along another choice in the method for the quantitation of the analytes, which is the use of an appropriate internal standard. Once the optimized conditions of the method are established, they must be validated to prove its reliability.

In this research, SPME coupled with GC/MS was used to quantitate halogenated anisoles present in wine at or below their olfactory thresholds. These compounds, as previously stated in Chapter 1.B, make the wine undrinkable, due to the foul aroma and undesired taste even in such low concentration (low ng L^{-1}). Therefore, a method was developed, optimized, and validated to quantitate these compounds. The conditions of the method optimization and validation are listed in the following sections.

A. Selection of Internal Standards

Since 2,4,6-trichloroanisole, 2,3,4,6-tetrachloroanisole, 2,4,6-tribromoanisole, and pentachloroanisole were analyzed, only two internal standards were investigated for quantitation. Trichlorotoluene (TCT) was first investigated because it was readily available and inexpensive. Later in the research, 2,4,6-Trichloranisole-d_5 (TCA-d_5) was explored and replaced TCT. Literature was reviewed and it was found that neither of these two compounds naturally occurs in wine. The details why TCA-d_5 was ultimately employed over TCT are discussed in Chapter 4.

B. Preliminary Experiments

Preliminary research of these analytes was performed and the initial procedure included sample incubation at an agitation speed of 500 rpm for five minutes, followed by extraction for 30 minutes at 55 °C at the same agitation speed. The detection conditions are described in Chapter 2.F. One vial of synthetic model wine solution was spiked with 1 µg/L of TCA, TeCA, TBA, PCA, and TCT and analyzed to identify acceptable retention times and resolution. This data also determined which ions would be collected for selected ion storage (SIS) for quantitation.

SIS is often confused with selected ion monitoring (SIM). Both methods when used correctly, provide increased sensitivity. When SIM is used, only a single or small selected ion range is monitored. A loss of sensitivity occurs when the *m/z* range is increased to adequately collect enough ions to identify the mass spectrum of the analyte in SIM. SIS, in contrast, is capable of storing a 30-50 mass range without a loss of sensitivity [22]. While SIS is used, no background ions are accumulated within the trap

and the storage capacity is then only dedicated to the ions of interest. This provides a cleaner spectrum and increases sensitivity which is ideal for ultra-trace analysis.

The preliminary precision, limit of detection (LOD, signal-to-noise ≤ 3), and limit of quantitation (LOQ, signal-to-noise ≤ 10) were determined to lower the effective range of the standard addition curve and to identify whether the samples needed to be run in triplicate. Once the results were determined and accepted, six vials containing 3.0 g NaCl with 10 mL of model wine (12% ethanol, 7.0 g L^{-1} tartaric acid, pH 3.4) were prepared and spiked accordingly with 10, 20, 30, 40, 50, and 60 ng L^{-1} of each haloanisole and 50 ng L^{-1} of TCT. These standard addition curves were used during the optimization process in order to determine whether an increase in instrumental response versus analyte response occurs.

During the optimization process, the model wine was spiked with 40 ng L^{-1} of each haloanisole and 50 ng L^{-1} of the internal standard TCT, which was labeled as the synthetic working solution one (SWS#1). After optimization, TCT was discarded and TCA-d_5 was used as the internal standard. The model wine solution used thereafter was spiked with 40 ng L^{-1} of each haloanisole and 30 ng L^{-1} of TCA-d_5, labeled as synthetic working solution two (SWS#2). All extractions were done in triplicate where appropriate.

C. Sampling Parameters

The goal of altering the sampling parameters was to transfer the largest amount of analyte onto the fiber to increase the overall sensitivity, limit of detection, and limit of quantitation. Based on preliminary results, the parameters were adjusted above and

below the standard values in order to determine if there was an increase (or decrease) in extraction. An autosampler was also implemented and helped alleviate variability because of consistent sampling and injections when performing SPME. Experimental conditions of injection temperature and time, extraction temperature and time, salting out, pH, sample volume, and ethanol dilution are further discussed.

1. Injection Temperature and Desorption Time

The temperature of the injection port was investigated to determine if all of the adsorbed analytes on the fiber were completely desorbed. Any residual analytes on the fiber will reduce extraction efficiency and possibly contaminate subsequent samples. Four SWS#1 samples were prepared, and injected individually at 240 °C, 250 °C, 260 °C, and 270 °C with an empty laboratory air blank vial, free of haloanisoles and TCT, between each SWS#1 injections. The temperature that provided the highest analyte response and lowest residual carry-over was determined and subsequently applied.

Once the optimal injection temperature was implemented, the necessary time the fiber must remain in the injection port for complete desorption was investigated. As described above, the conditions for the best extraction and desorption process were studied to determine how long the fiber must remain in the injection port for complete desorption. Three SWS#1 samples were prepared and desorbed individually for 5 minutes, 7 minutes, and 10 minutes at the previously optimized extraction temperature with a laboratory air blank between SWS#1 injections to monitor and eliminate analyte carry-over in consecutive

experiments. The time required for complete desorption of the fiber was identified and applied for each subsequent run.

2. Extraction Temperature

The duration of exposure the fiber has in the headspace is strongly influenced by the extraction temperature. Usually, an increase in extraction temperature will usually increase the mass transfer of the analytes to the fiber thereby decreasing the time required for the SPME fiber to reach equilibrium with the sample matrix and the headspace. Extraction temperatures of 40 °C, 50 °C, 55 °C, 60 °C, and 70 °C were employed to obtain the optimum temperature for extraction of each haloanisole in the SWS#1 samples. Since there was not a unanimous optimum extraction temperature, a compromise was made for the best overall temperature and was applied to the method.

3. Extraction Time

The aim of the evaluation of extraction time was to determine the time required for the analytes between the sample matrix and the stationary phase of the SPME fiber to reach equilibrium. The more volatile compounds saturate the headspace more quickly than the analytes with lower vapor pressures. This may cause a lower response the analytes demonstrate with lower vapor pressures. The DVB/CAR/PDMS fiber used in this study has been shown to have a slow saturation, due to the porosity of the coating that enables it to retain a larger amount of analyte [11].

Optimization of the extraction time was conducted to determine the most efficient time required to get an accurate representation of analytes present in the sample. In this study, exposure times of 30, 60, and 90 minutes were investigated for SWS#1 samples. The time requirement for the highest analyte response was identified and implemented from there on.

4. Salting Out

The technique of "salting out" is frequently used prior to extraction when analyzing volatile compounds in wine. Salting out occurs when a non-competitive ionic salt is added to the liquid matrix, thereby increasing the ionic character of the solution. This approach essentially drives the less polar volatile compounds from the water into the headspace in an effort to solvate the ions. This results in a higher percentage of volatile analytes in the headspace for extraction.

There are numerous types of non-competitive ionic salts available for this process: sodium chloride [11,13,17,23], potassium hydrogen carbonate [16], and a mixture of ammonium sulfate and sodium dihydrogen phosphate [15]. The research described herein used sodium chloride, due to its uncomplicated preparation and common usage for this process. The salt was heated for 24 hours at 250ºC to drive off all water and volatile organics. The resulting anhydrous salt was stored in a desiccator at room temperature. Four SWS#1 samples were prepared with 0, 1.0, 2.0, and 3.0 g of NaCl. The highest solute area response was identified and that amount of NaCl was used from there forth.

5. pH

pH can be an important parameter to investigate when evaluating extraction efficiency. Phenols, the intermediate to anisoles, ($pK_a \approx 10$), have been found to extract more efficiently in an acidic environment. The pH corresponding to the maximum extraction efficiency was determined by altering the sample pH with sodium hydroxide and hydrochloric acid from pH 2-9 in increments of one. The pH with the highest extraction efficiency was used thereafter.

6. Sample Volume/Vial Volume

Sample volume/vial volume (sV/vV) is an important variable to investigate when headspace extraction is analyzed. Ideally the liquid sample, gaseous headspace and fiber will contain equal concentrations of desired analytes at the end of the extraction. For that reason different volumes of the sample were investigated to determine the highest mass transfer, with the vial volume held constant at 20 milliliters.

7. Ethanol Dilution

Ethanol is the main volatile component present in wine, and is the main inhibitor against volatile analytes for the adsorption on the SPME fiber. Solutes which are soluble in ethanol will tend to remain dissolved in solution and have a decreased response on extraction in the gas phase. Consequently, a decrease in ethanol content will improve the analyte response as more will be collected. To examine the ethanol effects, the model wine samples were diluted to 8%, 9%,

10%, and 11% ethanol from the original 12% v/v model wine and then spiked accordingly to the SWS#1 analyte amounts. The opposing effect that ethanol has on the analytes was evaluated by increasing the ethanol amount of the original 12% v/v model wine to 13%, 14%, 15%, and 16% ethanol and spiked accordingly to see if a negative response occurs. Once the ethanol variation data was acquired, the following equation was implemented to normalize the previous data to determine the optimum ethanol amount during extraction with the highest analyte response:

$$\frac{sampleEtOH}{12\%EtOH} \times \frac{samplearea}{12\%EtOHarea} \qquad \text{Equation 3.1}$$

After the normalization to the diluted analyte area was calculated, the best compromise of sample dilution was determined and employed.

D. Validation of the Method

Method validation is an essential process that confirms the analytical method is acceptable for the proposed use. The results of validation will indicate whether the proposed method is reliable, consistent, reproducible, and accurate. The requirements for validation for an accurate quantitation of the haloanisoles in ultra trace amounts include linearity, specificity, precision, sensitivity, limit of detection, and limit of quantitation.

1. Linearity

Three linear standard addition curves were prepared using model wine, David Bynum Pinot Noir, and Carlo Rossi Chardonnay with the optimized method conditions. The analyte strengths were from 10-60 ng L^{-1} with an

increase in 10 ng L^{-1} increments of the haloanisoles and 30 ng L^{-1} of the internal standard TCA-d_5. As previously described in Equation 1.3, the comparison of the reference to analyte concentration was calculated by:

$$\frac{c_r}{c_{st}} = \frac{a_r}{a_{st}} \alpha_r$$

The resulting plots were analyzed for linearity by examining the coefficient of determination, R^2 and the equation of the line.

2. Specificity

The working solutions of the pinot noir, chardonnay, and model wine spiked accordingly with 40 ng L^{-1} of each haloanisole and 30 ng L^{-1} of the internal standard, TCA-d_5 and evaluated. The specificity was determined for each by calculating the resolution (R_s), capacity factor (k'), and number of theoretical plates (N and N^*) for the internal standard and solutes of interest. The equations are listed below and the appropriate measurements are included in Figure 3.1.

The resolution was measured by comparing the analyte peak (A) with the closest adjacent peak (B) in the chromatogram:

$$R_s = \frac{2\left(t_{r,B} - t_{r,A}\right)}{W_A + W_B}$$

where the width of the base peak, W_A and W_B, was determined by extending the tangent line down each side to the baseline. The capacity factor and number of

theoretical plates were calculated for each solute of interest shown by the following equations:

$$\text{Capacity factor: } k' = \frac{t_r - t_m}{t_m}$$

$$\text{Number of theoretical plates for symmetric peaks: } N = 16\left(\frac{t_r}{W_b}\right)^2$$

$$\text{Number of theoretical plates for asymmetric peaks: } N^* = 5.54\left(\frac{t_r}{W_{1/2}}\right)^2$$

$$\text{Peak Symmetry: } A_s = \frac{b}{a}$$

The variables contained in these expressions were described earlier in Chapter 1.E: Equations 1.12 for R_s, 1.5 for k', 1.11 for N and N^*, and 1.13 for A_s.

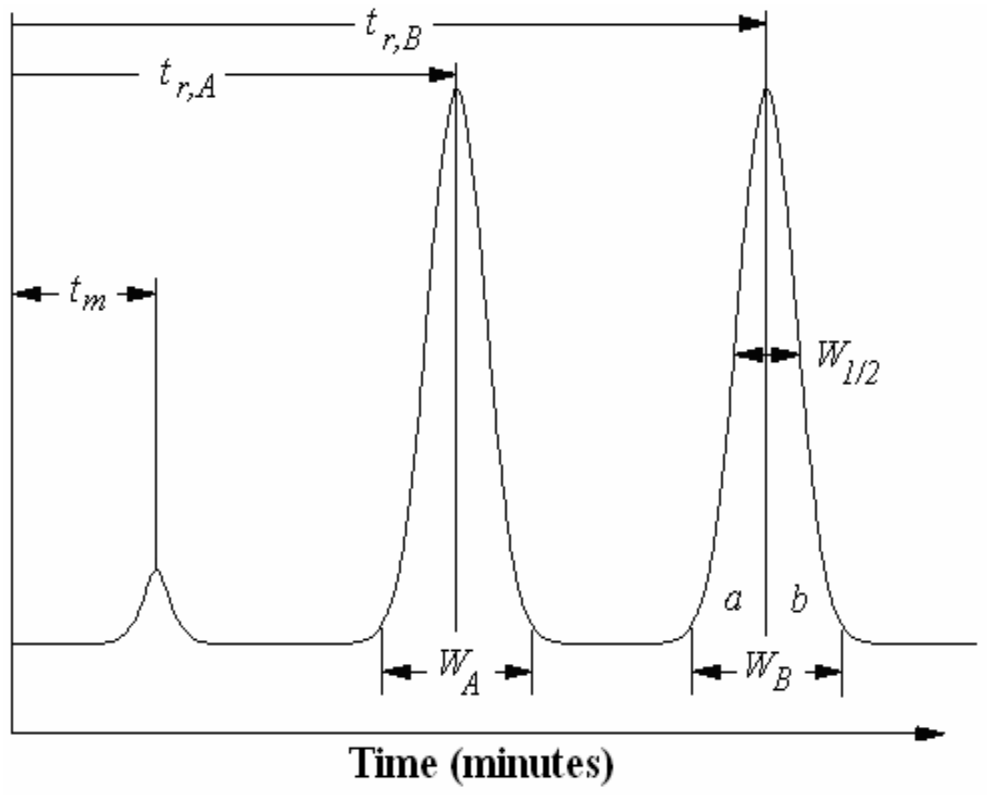

Figure 3.1: Measurements displayed on a generic gas chromatogram when calculating the resolution, capacity factor, number of theoretical plates, and symmetry of the peaks.

3. Precision

Precision is often referred to as repeatability or reproducibility of the results. Precision is determined by calculating the relative standard deviation, *RSD*. The relative standard deviation is represented as a coefficient of variation expressed as a percentage. The acceptable values of *RSD* are <10%. This study took five vials of equal concentration of SWS#1 and five of SWS#2 and the *RSD* were determined and compared.

The second evaluation of precision analyzed the variation between two standard curves of the same sample matrix and spiked concentration using the

same optimized method. The slopes and intensities were analyzed and evaluated for the proper precision.

4. Sensitivity

Sensitivity is measured by an increase in the signal per unit of concentration of each individual analyte. An accurate detectable signal requires a certain amount of particles to hit the detector for the true representation of that particular analyte concentration. Therefore, sensitivity is inversely related to scan speed when the total ion count (TIC) is analyzed, due to competition for the detector when a fast scan rate is permitted. Analogously, when SIS is implemented, only a selected ion range is viewed where the length of the scan rate could cause an under representation of the ions present at a particular retention time.

To test the sensitivity of the method, the scan rate was investigated to determine if there was a change in analyte response. Three SWS#1 samples were analyzed with scan rates of 0.22, 0.39, and 0.60 seconds/scan. Once the optimum scan rate was established, new linear standard addition curves were plotted and the increase of solutes was analyzed to determine if the increase in concentration followed a consistent trend by evaluating the slope and y-intercept.

5. Limit of Detection

The limit of detection (LOD) is defined as the lowest quantity of a substance that will yield a signal at least three times that of the adjacent noise.

The LOD represents the level at which the analyte is believed to be present, but not conclusively. From this any analytical method can only qualitatively state that the analyte is believed to be present.

6. Limit of Quantitation

The limit of quantitation (LOQ) is the lowest amount of an analyte that can be accurately and precisely measured with a signal that is at least 10 times the adjacent noise. A signal to noise (S/N) ratio of 10 or higher is to ensure that any error, within acceptable ranges, will not have a dramatic effect on the quantitative results.

Chapter IV

Results and Discussion

A. Identification of the Standards

The standards were identified by using one model wine solution spiked with one µg L^{-1} of each haloanisole and the internal standard (TCT) and compared against a model wine blank, which was free of the analytes. The mass range selected was 120 – 350 *m/z*. The compounds were identified by comparing the mass spectrum of a peak that was believed to be the desired solute against the Saturn software NIST library. The model wine chromatogram with the targeted peaks labeled can be seen in Figure 4.1 along with the mass spectra of each targeted analyte compared against the NIST library mass spectra in Figure 4.2 – 4.6 for TCT, TCA, TeCA, TBA, and PCA respectively.

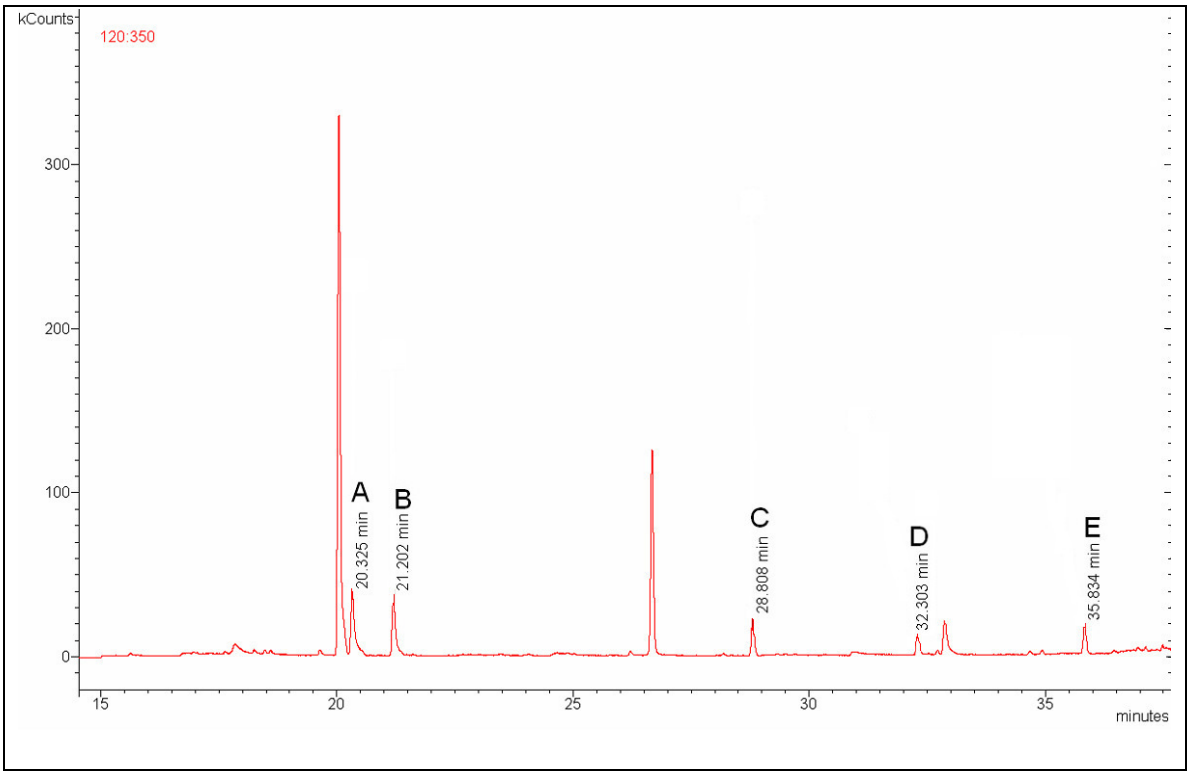

Figure 4.1: Chromatogram of a model wine solution spiked with 1 µg/L of each targeted analyte: (A) TCT, (B) TCA, (C) TeCA, (D) TBA, and (E) PCA.

The mass spectrum of the peak at 20.325 minutes in Figure 4.2, was compared against the NIST library TCT mass spectrum. The major mass spectrum peaks (*m/z* 123, 159, 161, 194, and 196) and the isotope distributions of TCT matched the NIST spectrum. The analyte that eluted at 20.325 minutes was assigned as TCT.

The mass spectrum of the chromatographic peaks of Figures 4.3 – 4.6 were investigated and compared against the NIST library mass spectrums for TCA, TeCA, TBA, and PCA as well. The major spectrum peaks matched and were labeled accordingly.

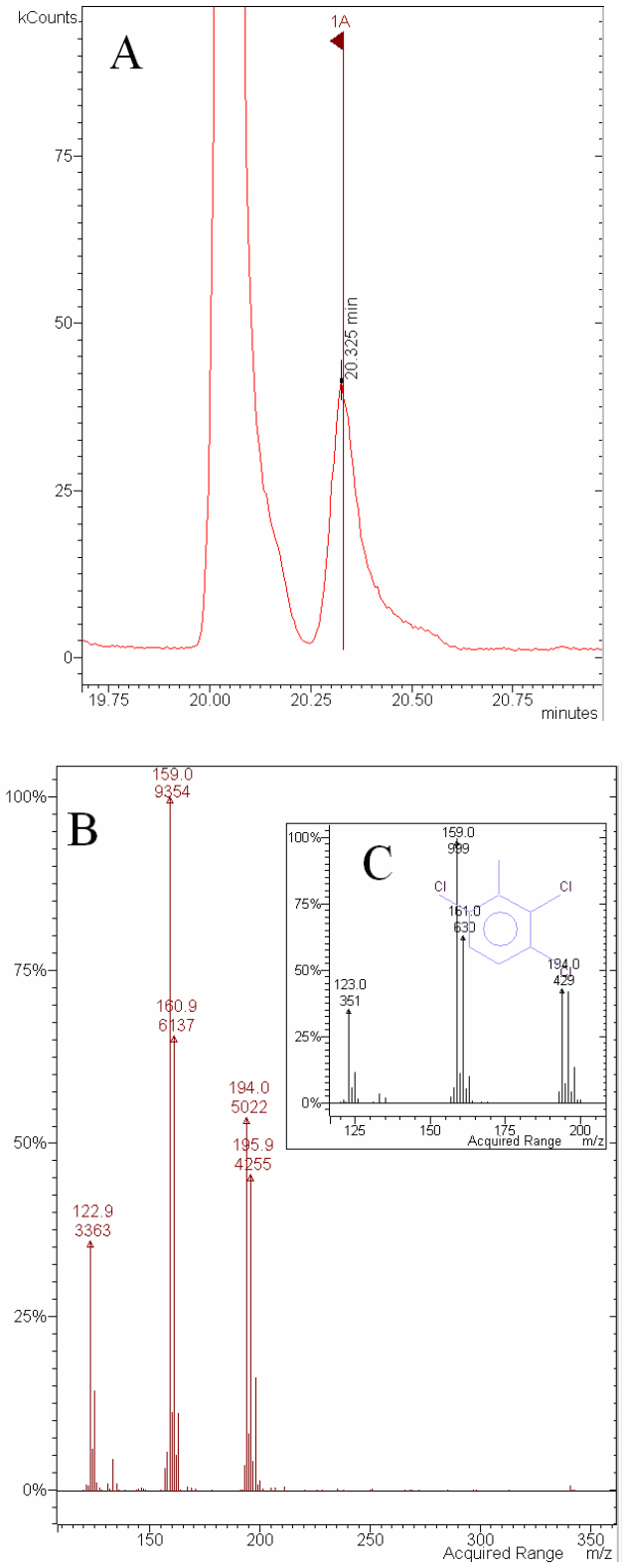

Figure 4.2: (A) TCT chromatogram peak, (B) mass spectrum of TCT, and (C) NIST library TCT mass spectrum for comparison.

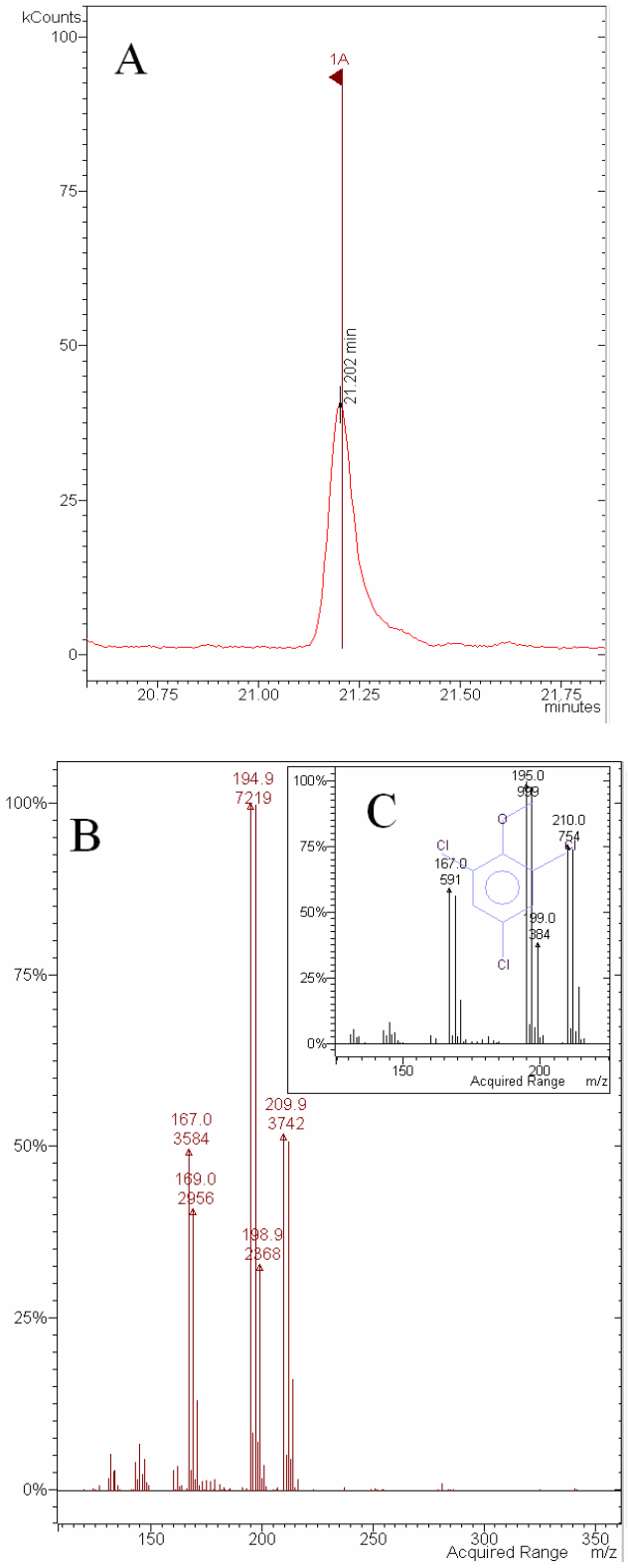

Figure 4.3: (A) TCA chromatogram peak, (B) mass spectrum of TCA, and (C) NIST library TCA mass spectrum for comparison.

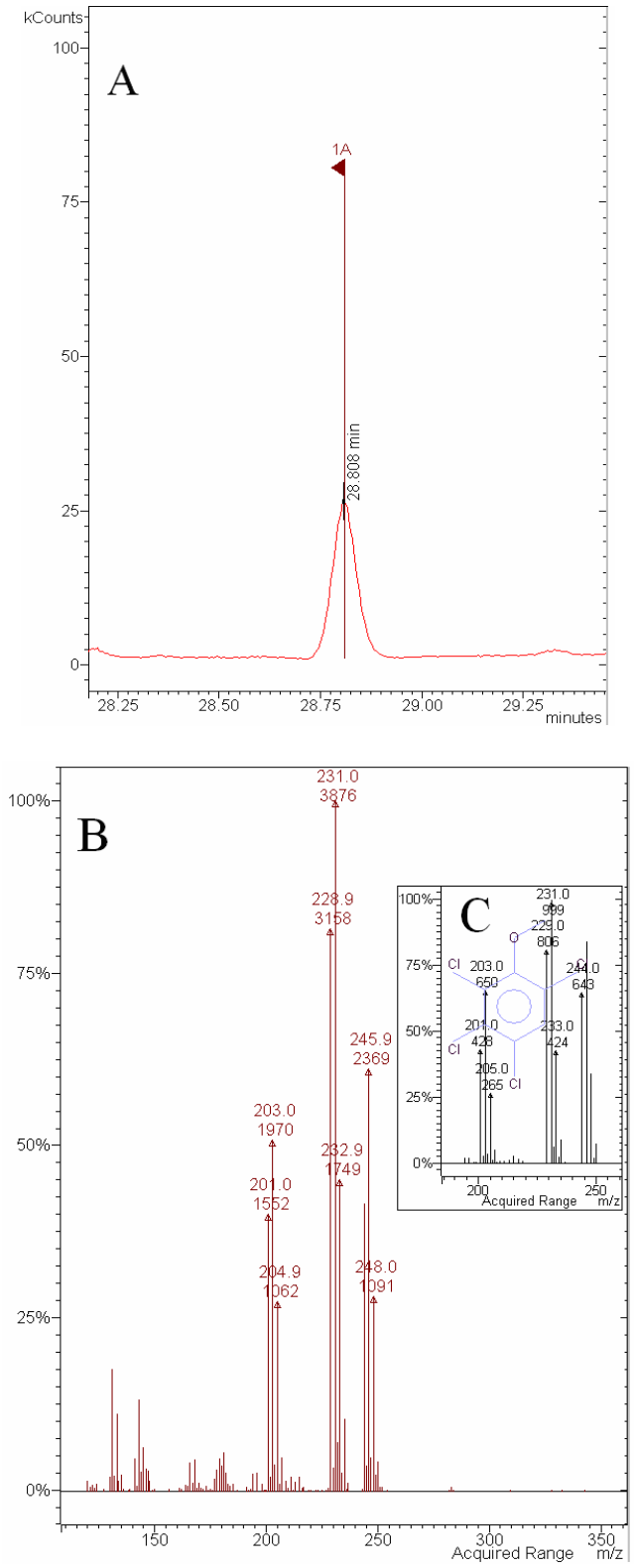

Figure 4.4: (A) TeCA chromatogram peak, (B) mass spectrum of TeCA, and (C) NIST library TeCA mass spectrum for comparison.

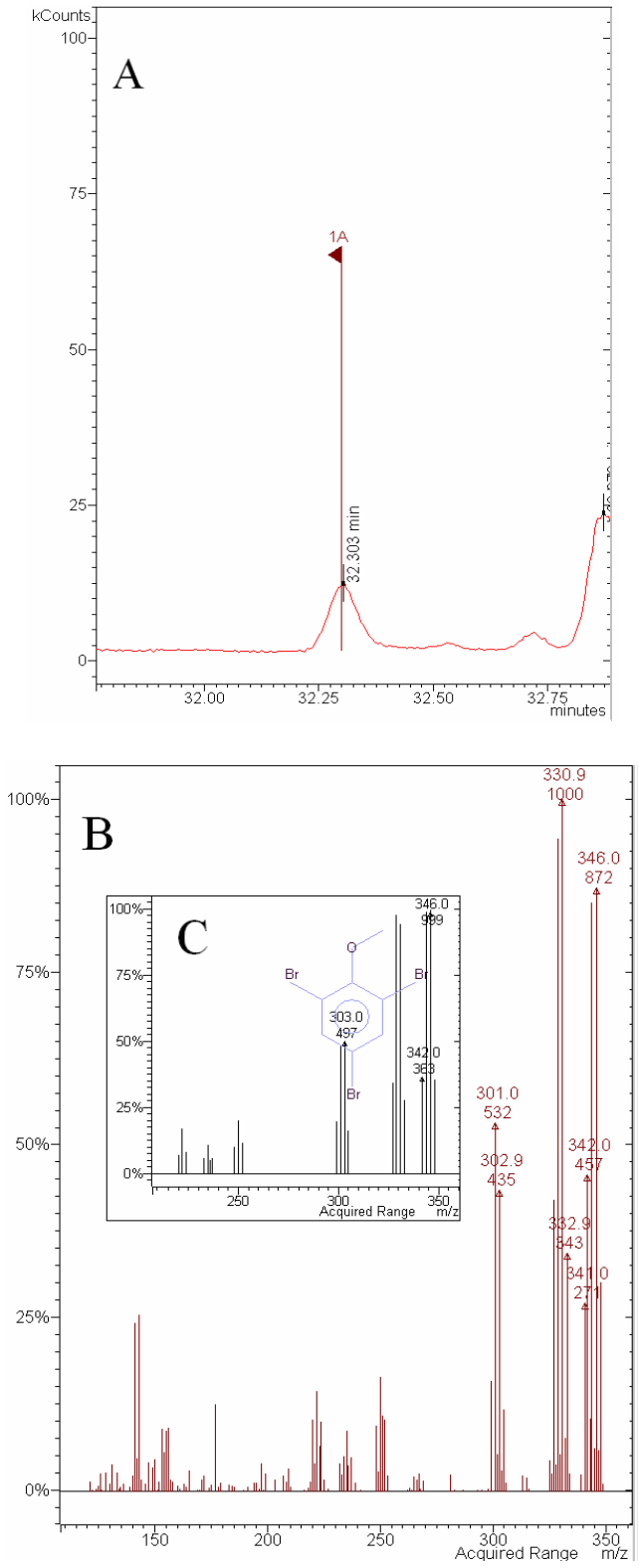

Figure 4.5: (A) TBA chromatogram peak, (B) mass spectrum of TBA, and (C) NIST library TBA mass spectrum for comparison.

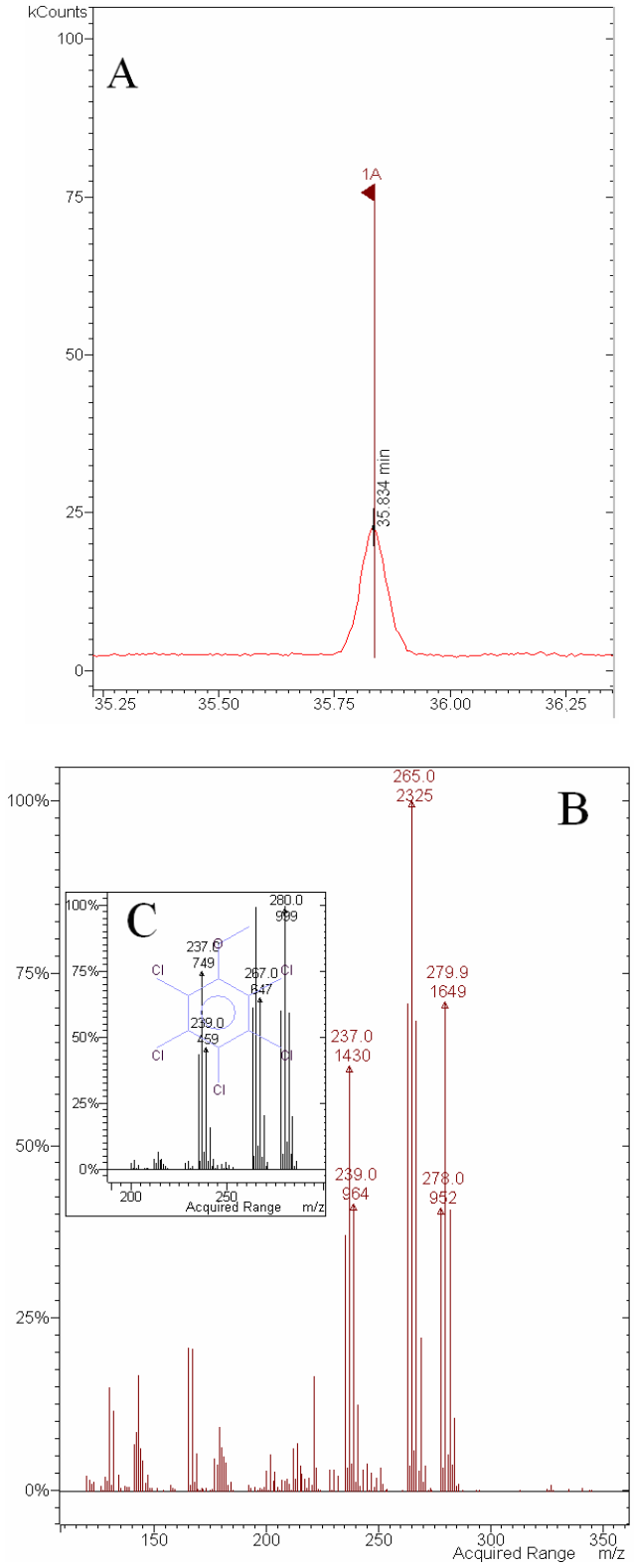

Figure 4.6: (A) PCA chromatogram peak, (B) mass spectrum of PCA, and (C) NIST library PCA mass spectrum for comparison.

B. Determination of the Quantitation Ions for SIS mode

As previously described in Chapter 3.B, SIS increases the sensitivity of the mass spectrometer by omitting the background ions from being stored within the ion trap, which decreases the adjacent noise level, and allows for the collection of ions that pertain only to the ions of interest. Usually the base peak of the spectrum is chosen for the quantitation ion, but the noise level surrounding the ions must also be investigated to determine if the S/N ratio is maximized. For that reason, the mass spectra of the five compounds were examined by comparing the most intense peaks within the mass spectrum.

The chromatogram of TCT is displayed in Figure 4.7 and includes the ions of *m/z* 159 and 161. The mass spectrum of TCT is contained in Figure 4.2, where the base peak of TCT is *m/z* 159 and clearly shows the natural isotopic ratio of ^{35}Cl to ^{37}Cl (3:1). Given that the signal-to-noise is much higher for *m/z* 159, and the noise levels of both ions were equal, the ion 159 was selected for the quantitation ion of TCT. To quantify TCT, the mass spectral parameters were a mass range of 150 - 200 with a SIS ion mass range of 158 - 163.

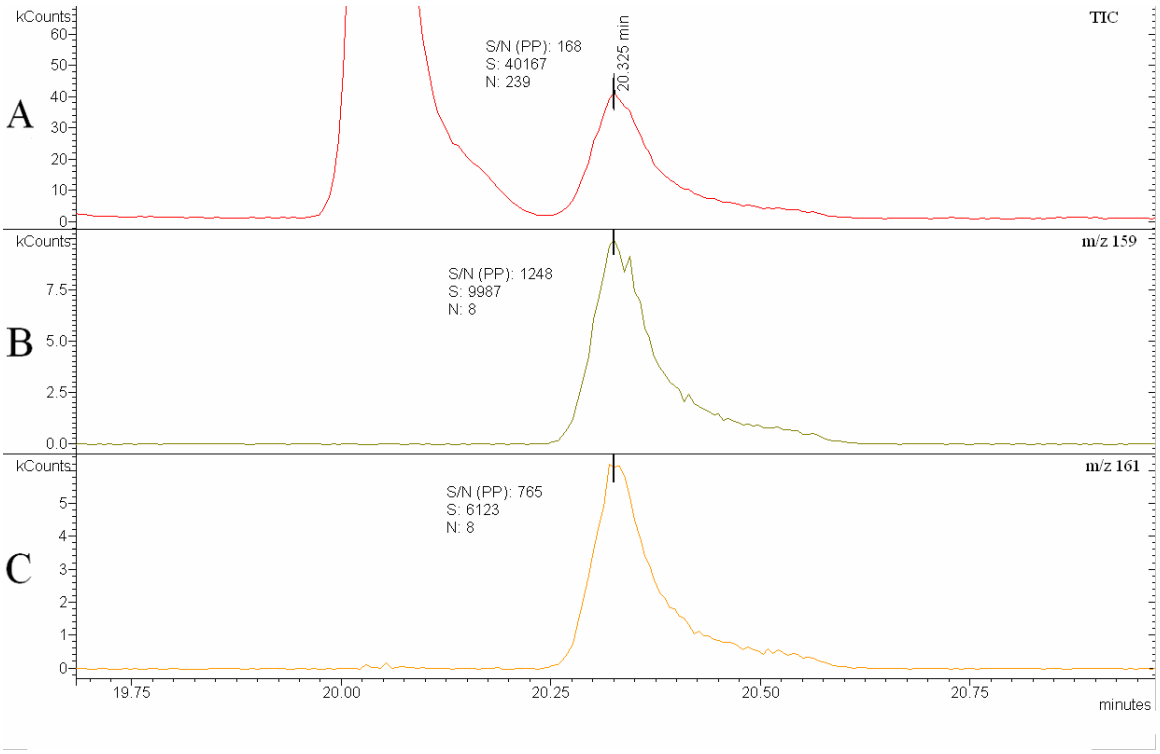

Figure 4.7: Chromatogram of TCT with ion peaks: (A) TIC mass range: 120-350 *m/z*, (B)SIS *m/z* 159 and (C) SIS *m/z* 161.

In Figures 4.8, 4.9, and 4.10 the S/N ratios were investigated for SIS quantitation ions for TCA, TeCA, and PCA. Since these three compounds all have chlorine isotopes, which have a natural abundancy of 3:1 ratio between ^{35}Cl and ^{37}Cl, the method of determining the SIS quantitation ion, mass ion range, and SIS ion range was determined as described in the previous paragraph. The quantitation ions, mass ranges, and SIS ion mass ranges selected for the three analytes are outlined in Table 4.1.

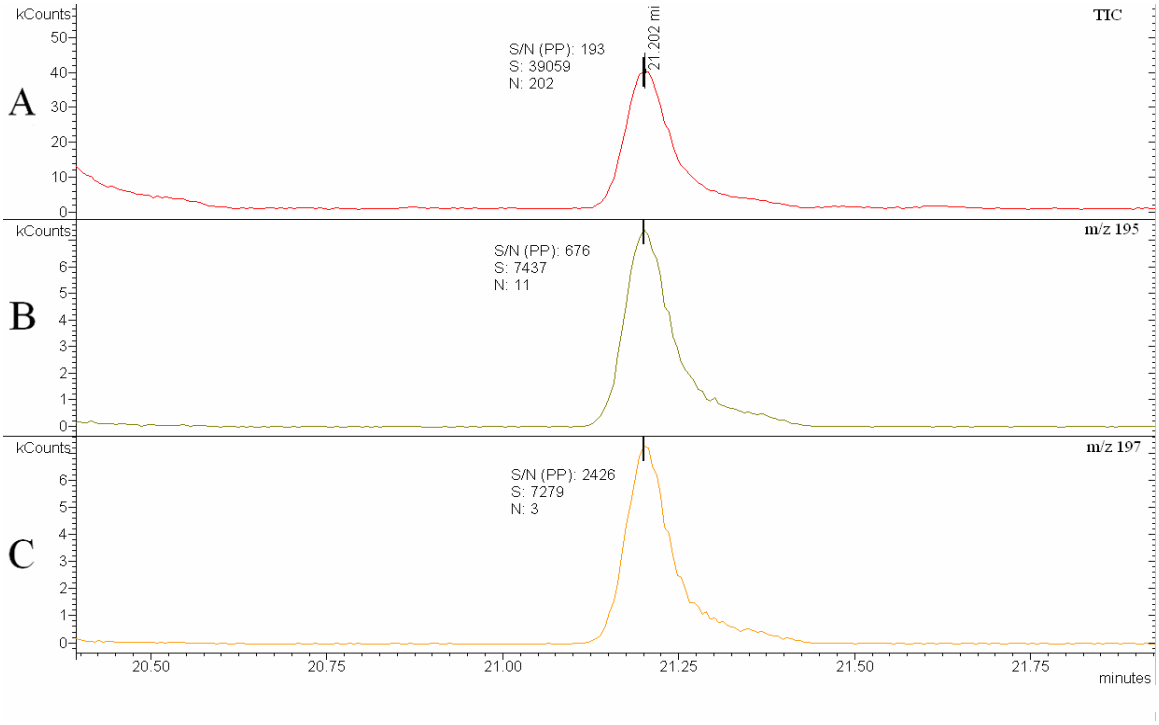

Figure 4.8: Chromatogram of TCA with ion peaks: (A) TIC mass range: 120-350 *m/z*, (B) SIS *m/z* 195 and (C) SIS *m/z* 197.

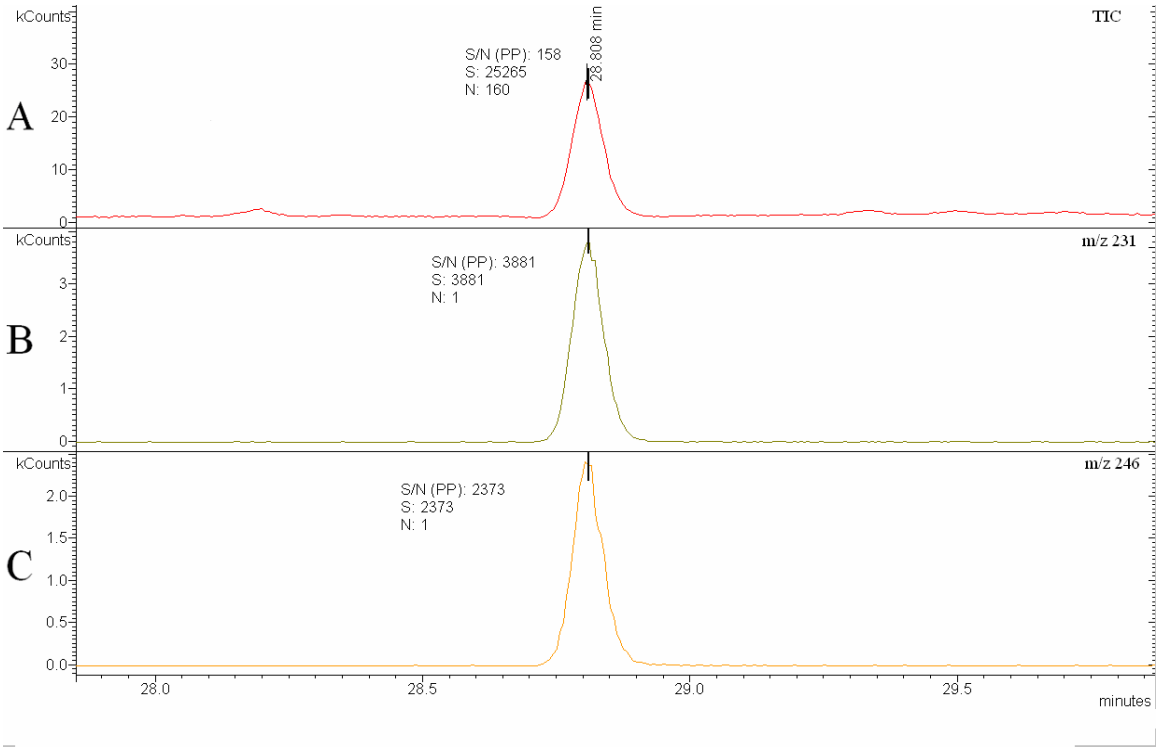

Figure 4.9: Chromatogram of TeCA with ion peaks: (A) TIC mass range: 120-350 *m/z*, (B) SIS *m/z* 231 and (C) SIS *m/z* 246.

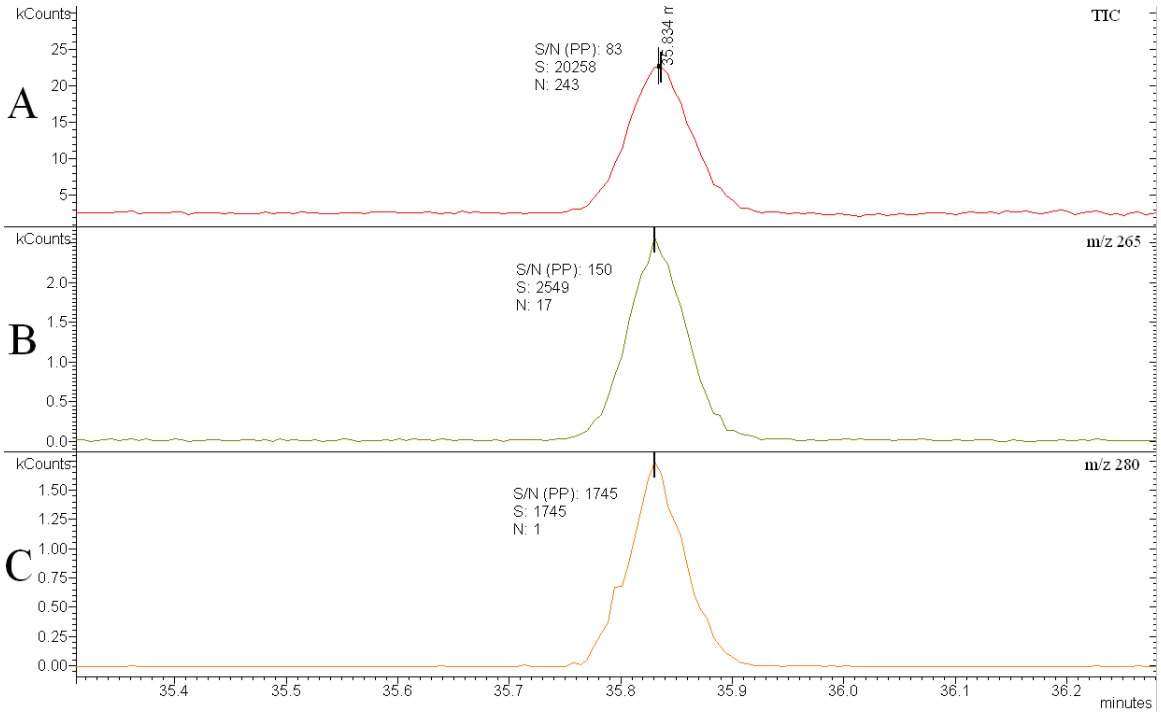

Figure 4.10: Chromatogram of PCA with ion peaks: (A) TIC mass range: 120-350 *m/z*, (B) SIS *m/z* 265 and (C) SIS *m/z* 280.

The quantitation ion for SIS of TBA was determined by investigating the three highest mass spectral peaks found in Figure 4.5. The quantitation ions selected were *m/z* 329, 331, and 346. Figure 4.11 contains the chromatogram of TBA. Bromine has a nearly 1:1 isotopic ratio of ^{79}Br to ^{81}Br and since there are three bromines on each TBA molecule, the bromine isotopic distribution ions selected were the most intense in the spectrum. In Figure 4.11 the noise level of ion with a *m/z* 329 has the highest intensity, but has a noise level of 4. When comparing the other two mass spectral peaks, ions 331 and 346. Both have a noise level of 1. Peak 331 had the highest S/N ratio and did not interfere with any other analytes and were selected for TBA, and the mass range selected was 320 - 335 with the SIS ion mass range of 327 - 333.

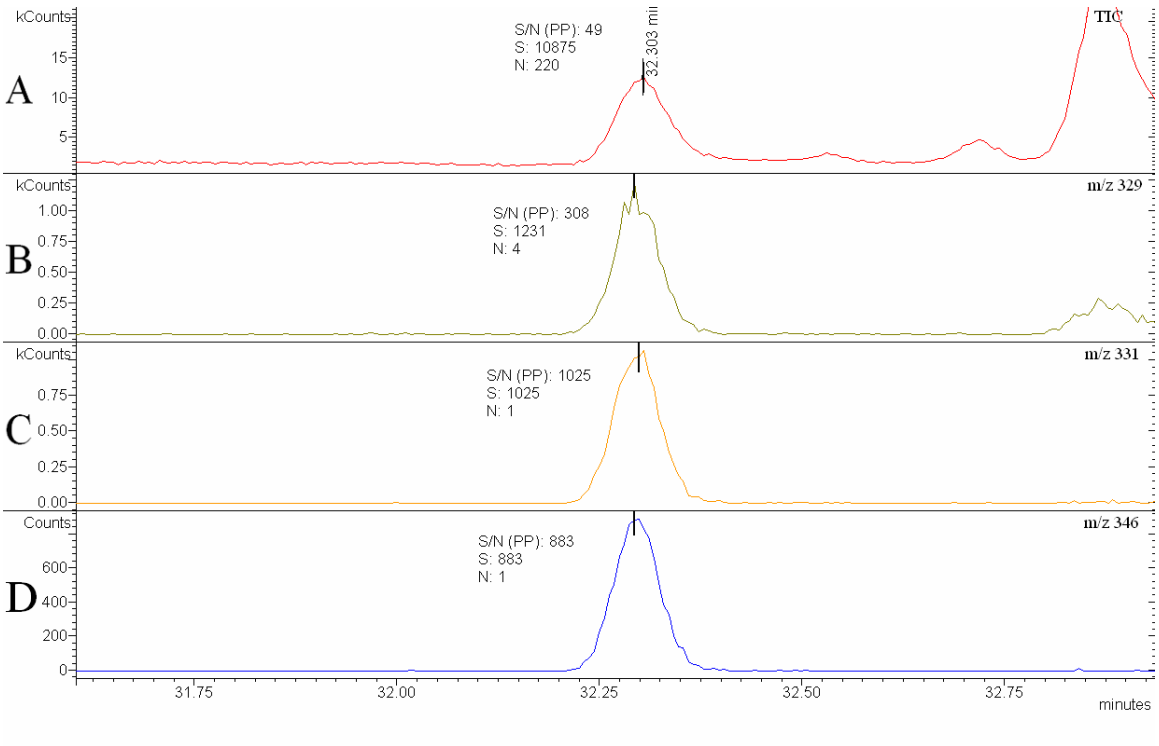

Figure 4.11: Chromatogram of TBA with ion peaks: (A) TIC mass range: 120-350 *m/z*, (B) SIS *m/z* 329, (C) SIS *m/z* 331, and (D) SIS *m/z* 346.

Table 4.1 contains a summary of the mass spectral analysis parameters.

Analyte	Segment Time(min)	Quant. Ion	Mass Range	SIS mass range
TCT	19.50 - 22.50	159 *m/z*	150 - 200 *m/z*	158 - 163 *m/z*
TCA	19.50 - 22.50	197 *m/z*	150 - 200 *m/z*	194 - 199 *m/z*
TeCA	22.50 - 30.00	231 *m/z*	210 - 250 *m/z*	228 - 236 *m/z*
TBA	30.00 - 34.00	331 *m/z*	320 - 335 *m/z*	327 - 333 *m/z*
PCA	34.00 - 37.00	280 *m/z*	275 - 286 *m/z*	277 - 284 *m/z*

Table 4.1: Summary of mass spectral analysis parameters.

C. Preliminary Experiments

The precision was calculated by spiking 55 mL of model wine to a final concentration of 40 ng L^{-1} of TCA, TeCA, TBA, PCA and 50 ng L^{-1} of TCT. 10 mL of

this spiked model wine were then distributed to five 20 mL vials with 3.0 g of NaCl and sealed. The resulting relative standard deviations of the vials are presented in Table 4.2.

Analyte	RSD (%)
Trichlorotoluene	6.39
Trichloranisole	1.30
Tetrachloroanisole	3.97
Tribromoanisole	5.46
Pentachloroanisole	6.09

Table 4.2: Precision of haloanisoles in model wine solution.

The relative standard deviations all fall within the acceptable ranges, <10%, but the internal standard, TCT, has the highest variation. Ideally, the internal standard should have the lowest variation between the analytes, because it directly affects the analysis of all the other analytes. A new internal standard would seem appropriate and is described in later sections.

The LOD and LOQ were determined with the preliminary method to discover the lowest amount of analytes that could be detected and quantified in red and white wines. The red wine was Carlo Rossi Cabernet Sauvignon and the white wine was Carlo Rossi Chardonnay. The LOD and LOQ of model wine were not analyzed, due to it being a synthetic solution and not containing any haloanisoles by contaminations. Table 4.3 summarizes the preliminary LOD and LOQ results.

Analyte	Red Wine		White Wine	
	LOD (ng L^{-1})	LOQ (ng L^{-1})	LOD (ng L^{-1})	LOQ (ng L^{-1})
TCA	3.0	5.0	3.0	5.0
TeCA	3.0	6.0	4.0	6.0
TBA	5.0	9.0	6.0	10.0
PCA	5.0	10.0	6.0	10.0

Table 4.3: Preliminary limit of detection and limit of quantitation of red and white wine.

The highest preliminary LOQ was for PCA at 10 ng L^{-1} for both wines, therefore this concentration was chosen as the effective lower concentration for the curves to make sample preparation easier. A model wine standard addition curve was then prepared using 10, 20, 30, 40, 50, and 60 ng L^{-1} of each haloanisoles and 50 ng L^{-1} of TCT. Listed below in Table 4.4 is the linear range, equation of the line, and the coefficient of determination, R^2.

Analyte	Linear Range (ng L^{-1})	Equation of the Line	R^2
TCA	10-60	y = 1.8689x + 0.042765	0.9868
TeCA	10-60	y = 1.0998x + 0.050994	0.9759
TBA	10-60	y = 0.38058x - 0.021514	0.9844
PCA	10-60	y = 0.48598x - 0.008958	0.9856

Table 4.4: Preliminary method model wine linear calibration data.

D. Sampling Parameters

1. Injection Temperature and Time

Injection port temperatures were investigated to determine if complete desorption of the analytes from the SPME fiber actually occurred. Four SWS#1 samples were prepared and injected individually at temperatures of 240 °C, 250

°C, 260 °C, and 270 °C with an empty laboratory air blank vial, free of TCT and haloanisoles, between each SWS#1 samples. The injection temperature was not taken past 270 °C due to the manufacturer's recommendation of not exceeding 270 °C. As observed in Figure 4.12, 270 °C had the highest analyte desorption with the lowest residual analyte carry-over for all analytes. An injection port temperature of 270 °C causes the stationary phase of the DVB/CAR/PDMS fiber coating to become the least interactive with the adsorbed analytes and yields the best desorption. Therefore, the injection port temperature was then changed to 270 °C.

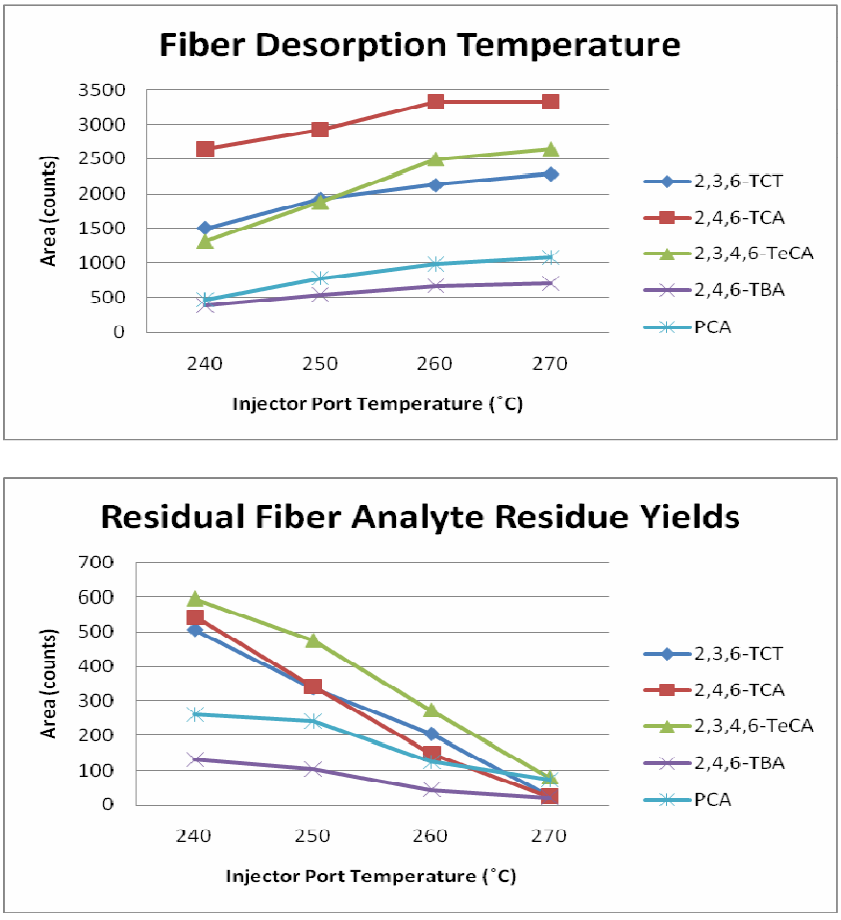

Figure 4.12: Effect of injection port temperature on analyte desorption (top) and analyte carryover (bottom).

The required time for the DVB/CAR/PDMS fiber to remain in the injection port to obtain the optimum desorption was then investigated. Three SWS#1 samples were prepared and injected individually for 5 minutes, 7 minutes, and 10 minutes at 270 °C with a laboratory air blank between each SWS#1 injection. As observed in Figure 4.13, 7 minutes provided the highest analyte response of TCA, TeCA, and PCA. TBA and TCT has a smaller analyte response from 7 to 10 minutes, but very minimal. When the analyte carry-over was analyzed, 7 minutes had the best desorption for only TCA, while 10 minutes was the best for TCT, TeCA, and PCA. TBA showed no analyte carry-over for either 7 and 10 minutes. To preserve the fiber lifetime, 7 minutes was selected as the best desorption time and applied to the method.

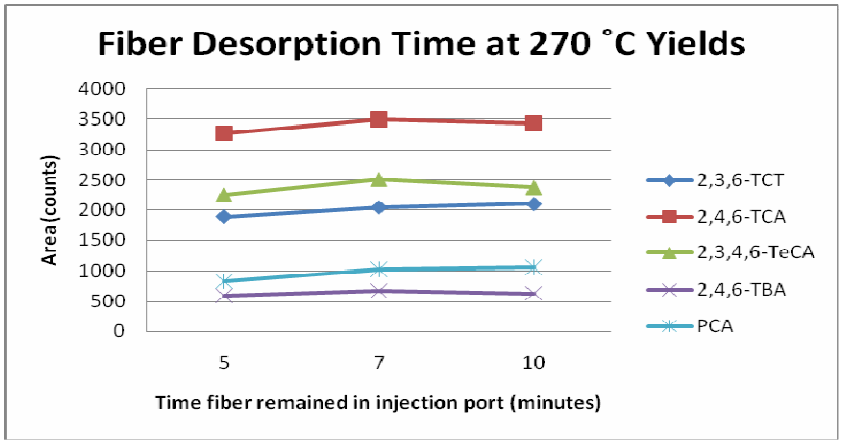

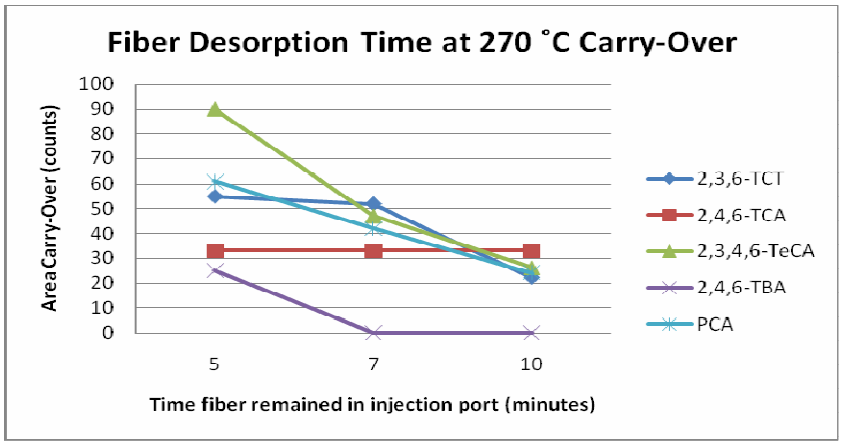

Figure: 4.13: Time required for optimal desorption of the analytes from the DVB/CAR/PRMS fiber at 270 °C.

2. Extraction Temperature

The temperature during extraction was investigated to acquire the highest mass transfer of the analytes to the fiber, which in turn decreases the time the SPME fiber requires to reach equilibrium with the sample matrix and the headspace. Five SWS#1 samples were prepared and extracted at 40 °C, 50 °C, 55 °C, 60 °C, and 70 °C. As Figure 4.14 shows, as the extraction temperature is increased, TeCA, TBA, and PCA have a higher mass transfer to the fiber. At 60 °C, TCA has the highest analyte response, but at 70 °C, it is not as readily absorbed to the SPME fiber. TCT has a better extraction at the lower temperatures, but it is the internal standard and the optimization process was for the haloanisoles. Therefore, a compromise was made and the optimum temperature for extraction was 60 °C and applied thereafter.

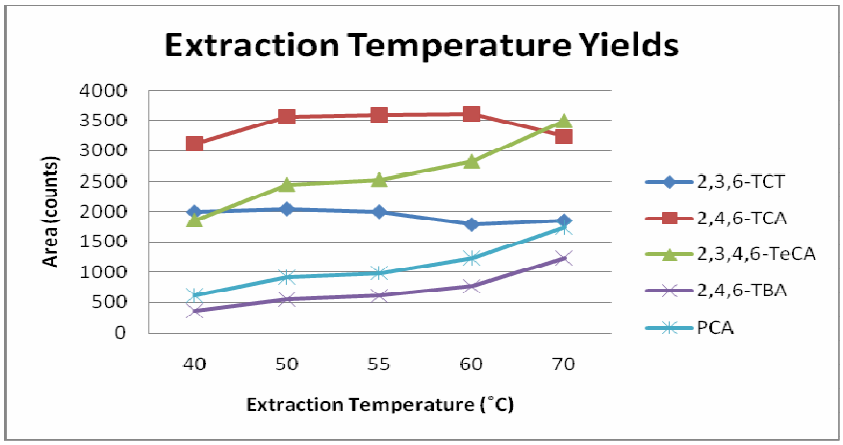

Figure 4.14: Extraction temperature effects on the DVB/CAR/PDMS fiber for extraction efficiency of analytes.

3. Extraction Time

The extraction time was evaluated to establish the optimal duration of exposure the fiber would require for the analytes to reach an equilibrium between the sample matrix and stationary phase of the DVB/CAR/PDMS fiber. Three SWS#1 samples were prepared and extracted for 30, 60, and 90 minutes. From Figure 4.15, none of the analytes were observed to reach an equilibrium between the fiber and the sample matrix. The analytes experience an increase in extraction almost linearly as the exposure time is increased. Since the response is almost linear for all the analytes, there is no false representation of analyte adsorption on the fiber. As time was not a factor, and the highest extraction was sought after, 90 minutes was chosen and implemented as the extraction time.

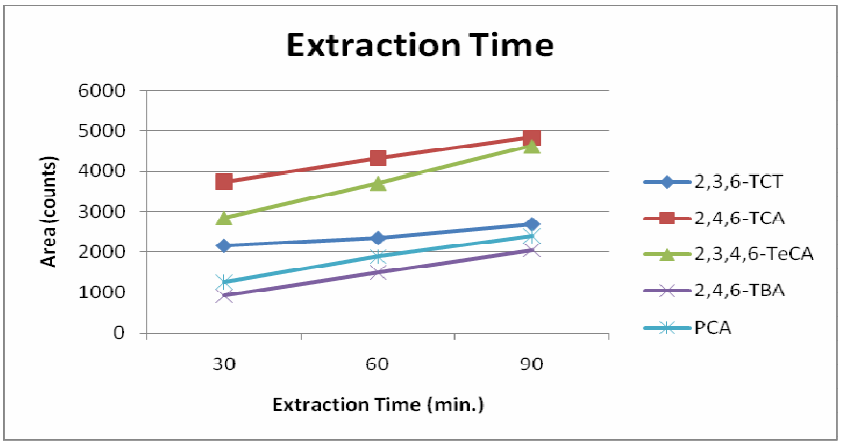

Figure 4.15: Effect of extraction time for saturation of the DVB/CAR/PDMS fiber for extraction efficiency of analytes at 70 °C.

4. Salting Out

Adding a noncompetitive ionic salt to the aqueous matrix prior to extraction drives out the less polar volatile compounds, this increases the transfer of volatile analytes to the headspace. The ionic strength of the solution was altered with 0, 1.0, 2.0, and 3.0 g of anhydrous NaCl to determine which salt concentration was required to get the highest response of the solutes. As Figure 4.16 indicates, 1.0 g of NaCl had the highest influence to drive the haloanisoles into the headspace. TCT extracts the best with no salt addition, but as previously stated in Section C.2, the optimization process is for the haloanisoles, and thus 1.0 g of NaCl was applied to the extraction method.

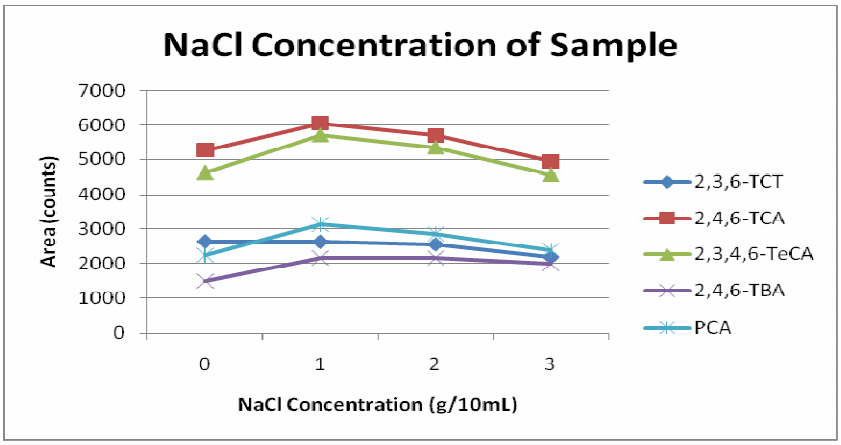

Figure 4.16: Influence of salt addition on extraction efficiency at 70 °C for 90 minutes.

5. pH

The pH of the sample was altered to determine if an acidic or basic environment will cause the haloanisoles to travel into the gas phase any faster. Eight SWS#1 model wine samples were prepared and the pH was altered with sodium hydroxide and hydrochloric acid from 2-9, in increments of one. Figure 4.17 indicates the sample pH has no effect on the extraction of haloanisoles. For that reason, the pH was kept at 3.4 for the model wine and the commercial wine samples pH was not altered.

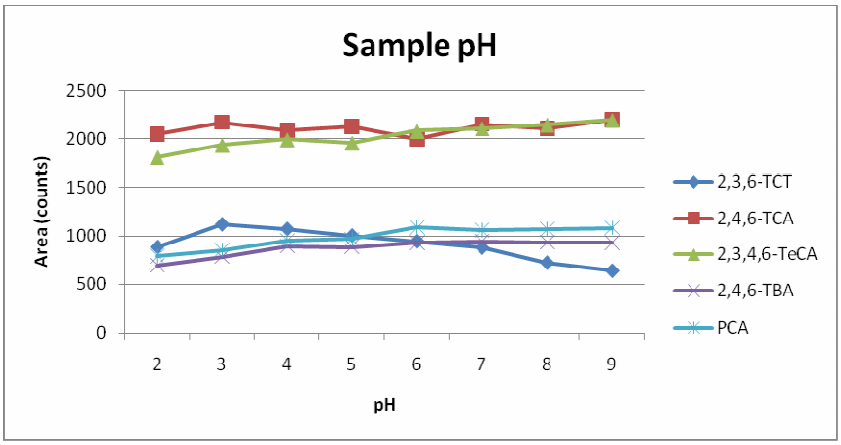

Figure 4.17: Effect of pH of sample on extraction efficiency at 70 °C for 90 minutes with 1.0 g NaCl.

6. Ratio of Sample Volume/Vial Volume

To achieve the optimal ratio, a 20 mL vial was used in all experiments and the volumes of the SWS#1 samples were only altered. In Figure 4.18, the sV/vV ratio of 1:1 had the best extraction for all the analytes. Due to the mass transfer of analytes to the headspace occurring at a constant rate, and a smaller headspace with a larger sample volume to pull from will saturate the gaseous headspace much quicker.

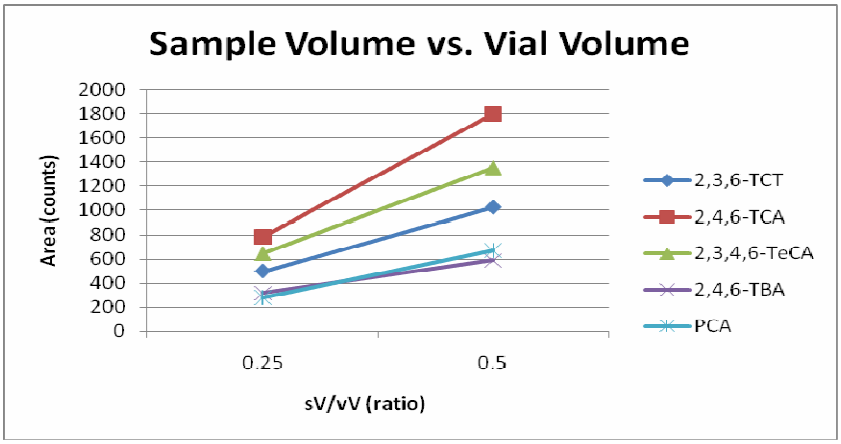

Figure 4.18: Effect sample volume/vial volume has on extraction efficiency at 70 °C for 90 minutes with 1.0 g NaCl per 10 mL model wine.

7. Ethanol Dilution

There is a competition between the compounds for binding to the SPME fiber, given the fibers fixed volume. Ethanol is the main volatile component of the aqueous system and the primary culprit for preventing haloanisoles from binding onto the fiber. The sample dilution profiles are shown in Figure 4.19, where the samples were diluted to an 8% - 11% ethanol content, from the original 12% v/v model wine solution, and then spiked accordingly to the SWS#1 analyte amounts. When further examining the role ethanol has on extraction, it was observed that the more ethanol the sample contains drastically reduces the amount of analyte adsorbed to the fiber (Figure 4.19). By decreasing the amount of ethanol in the sample by dilution with water, there was an increase in the amount of analyte adsorbed onto the fiber.

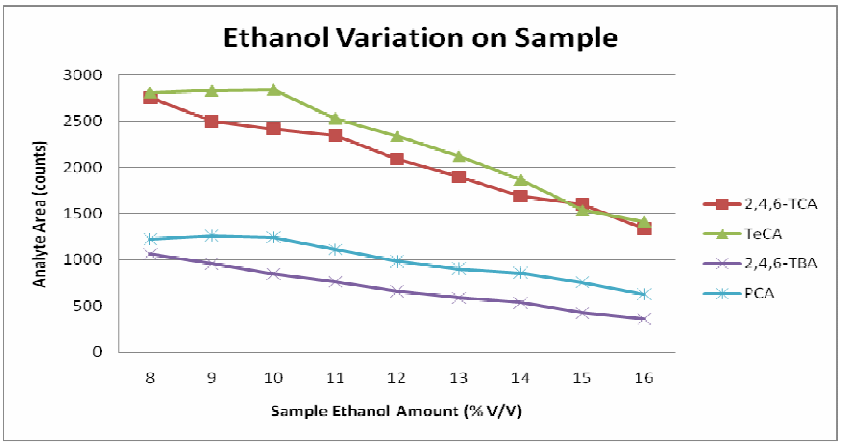

Figure 4.19: Effect of ethanol concentration on extraction efficiency at 70 °C for 90 minutes with 1.0 g NaCl per 10 mL model wine.

The data in Figure 4.19 was applied to Equation 3.1. This equation normalized the data and calculated the optimum ethanol amount that yielded the highest analyte response as shown in Figure 4.20. An ethanol content of 11% v/v

was determined to be the optimal amount where all future samples were adjusted to this ethanol content.

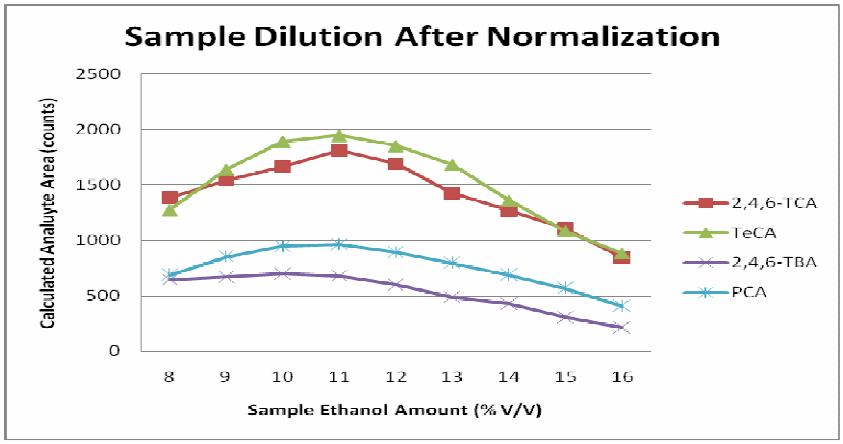

Figure 4.20: Effect of ethanol content and dilution effect on extraction efficiency of haloanisoles.

E. Selection of Internal Standards

The peak symmetry and precision of TCT was evaluated after optimization to determine if it had improved with the enhanced sampling conditions. As shown in Figure 4.21, the quantitation ion *m/z* 159 of TCT, used for quantitation of the haloanisoles, tails twice the width of the peak if it followed a Gaussian shape. This tailing effect unfortunately added uncertainty when calculating an accurate ratio.

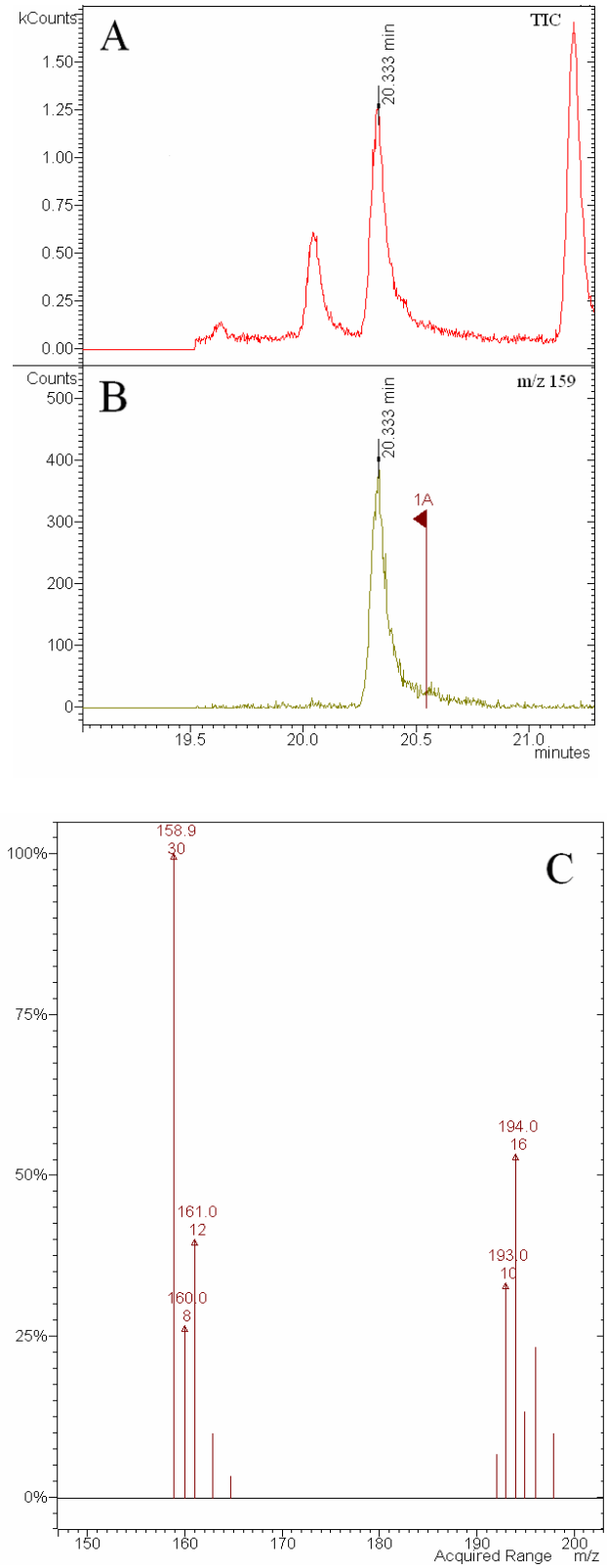

Figure 4.21: (A) Chromatogram of TCT indicating peak tailing (B) quantitation ion peak *m/z* 159 (C) mass spectrum of TCT tailing portion of the peak.

The precision was investigated next and compared to the preliminary calculations. Five SWS#1 samples were prepared and analyzed with the optimized method conditions. Details of the results are summarized below:

Compound	Model Wine Precision (n = 5) R.S.D. (%)		
	Conc. (ng L^{-1})	Preliminary Method	Optimized Method
TCT	50	6.4	17.0
TCA	40	1.3	1.4
TeCA	40	4.0	1.4
TBA	40	5.5	2.3
PCA	40	6.1	2.9

Table 4.5: Precision of preliminary and optimized methods.

After the results were evaluated, it was found that TCT under optimized conditions had a RSD of 17.0%, and is 2.66 times higher than the preliminary value, thus rendering TCT as an inappropriate internal standard. TCT was replaced by isotopically labeled TCA, 2,4,6-trichloroanisole-d_5, and will chemically behave in the same manner as undeuterated TCA.

The peak identification of TCA-d_5 was investigated by using a model wine spiked with 500 ng L^{-1} of TCA-d_5 and another model wine blank (no spiking) to compare against. The mass range selected was set to 150 – 250 *m/z*. The compound was identified by analyzing the expected mass spectrum and relative intensities of TCA-d_5, and to ensure that TCA did not contaminate the standard. The chromatogram of TCA-d_5 is included in Figure 4.22 along with its mass spectrum.

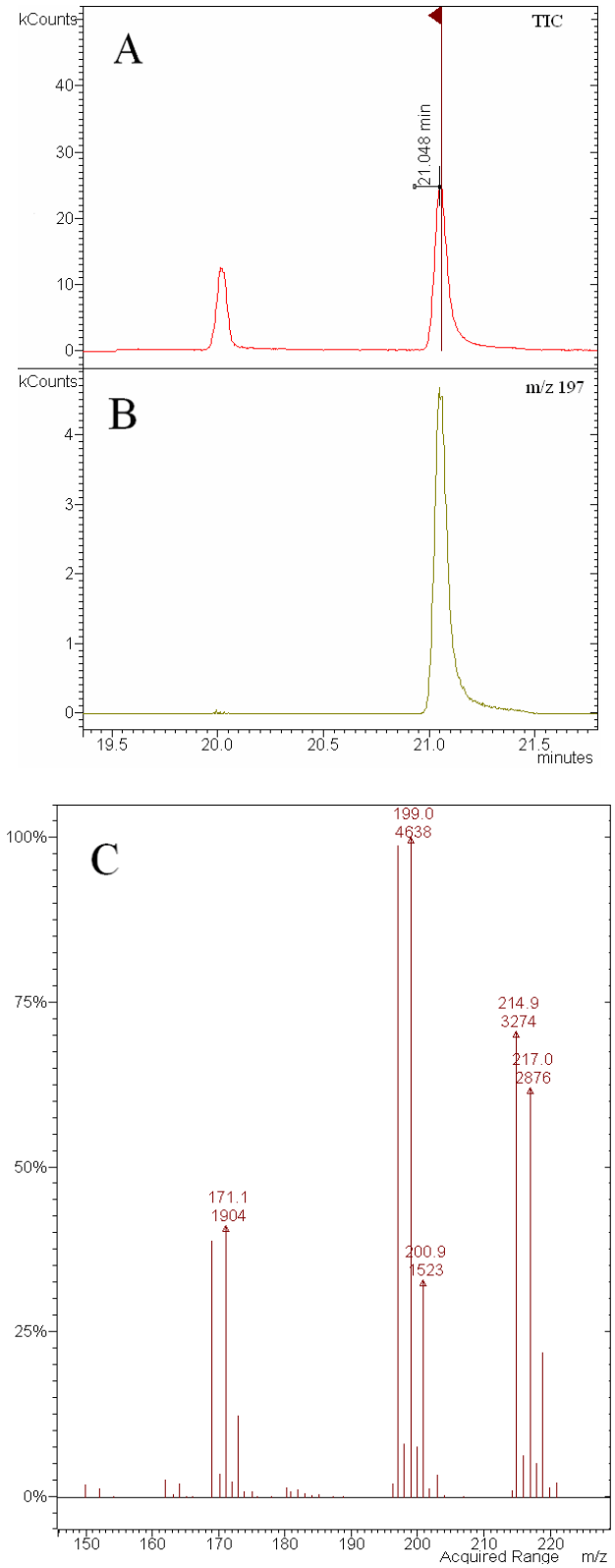

Figure 4.22: (A) Chromatogram of TCA-d_5 peak (B) SIS ion peak *m/z* 197, and (C) mass spectrum of TCA-d_5.

Figure 4.23 contains the chromatogram of TCA-d_5 and TCA. The quantitation ions of *m/z* 197 and 215 were investigated. The chromatographic resolution between TCA-d_5 and TCA needed improvement. For that reason, referring back to Figure 4.22, the base peak of TCA-d_5 was *m/z* 197 followed by *m/z* 199. From Figure 4.23, the ion of 197 of TCA-d_5 interferes with the TCA 197 quantitation ion peak, and 199 would have the same effect. To provide adequate resolution the mass spectrometer was used and the quantitation ion for TCA was changed from *m/z* 197 to *m/z* 195. The molecular ion peak of TCA-d_5 *m/z* 215 did not interfere with any other compound and was selected for the quantitation ion for the internal standard TCA-d_5. Therefore, the segment time for TCA-d_5 was 19.50 – 22.50 minutes, with the quantitation ion of *m/z* 215, mass ion range of *m/z* 150 - 225, and SIS ion range of *m/z* 214 - 222.

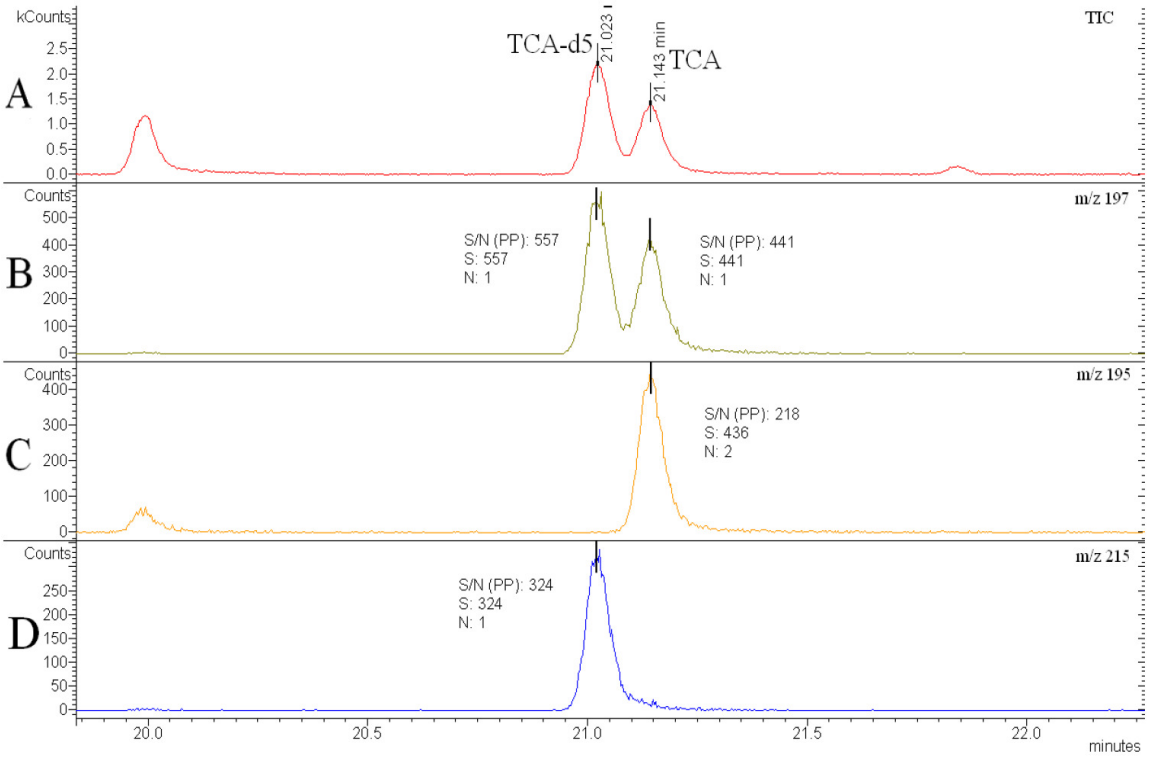

Figure 4.23: Chromatogram of TCA-d_5 with ion peaks of *m/z* 197 and 215, and TCA *m/z* 195.

F. Validation of the Method

1. Linearity

Three standard addition curves were prepared using model wine, David Bynum Pinot Noir, and Carlo Rossi Chardonnay with the optimized method conditions to validate the linearity of the curves of each sample matrix (synthetic, red, and white wine). The analyte strengths were from 10-60 ng L^{-1} with an increase in 10 ng L^{-1} increments of the haloanisoles, and the internal standard 2,4,6-TCA-d_5 held constant at 30 ng L^{-1}. The peak area of analyte/peak area of internal standard was plotted versus amount of analyte/amount of internal standard in Figure 4.24 for model wine. The resulting plots were analyzed for linearity, and are summarized in Table 4.6. The coefficients of determinations for all the plots were satisfactory.

Benzene, 1,3,5-trichloro-2-methoxy-
Curve Fit: Linear, Origin: Ignore, Weight: 1/nX2
Resp. Fact. RSD: 15.70%, Coeff. Det.(r2): 0.992656
y = +1.0107x +0.1968

Benzene, 1,2,3,5-tetrachloro-4-methoxy-
Curve Fit: Linear, Origin: Ignore, Weight: 1/nX2
Resp. Fact. RSD: 8.127%, Coeff. Det.(r2): 0.986779
y = +1.0919x +0.0839

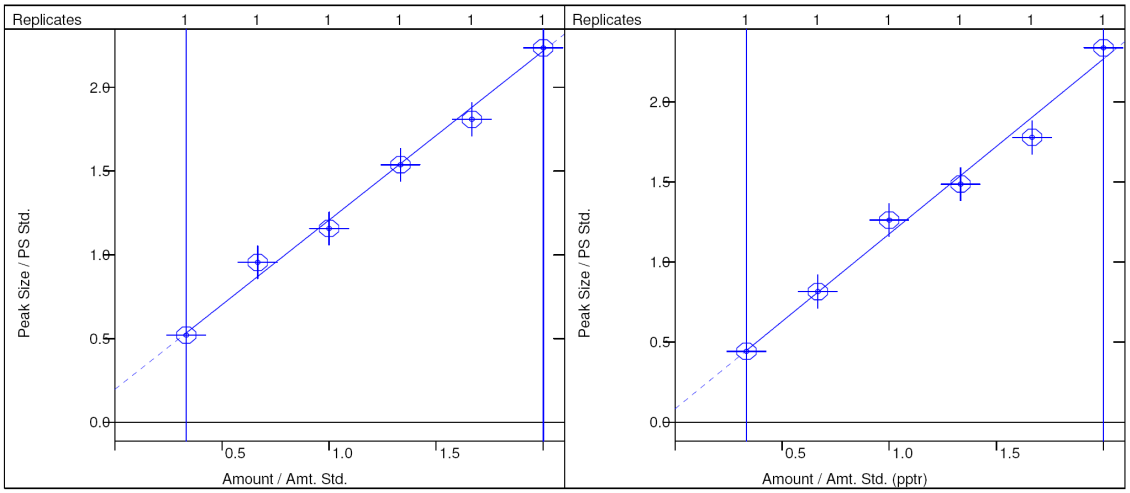

Benzene, 1,3,5-tribromo-2-methoxy-
Curve Fit: Linear, Origin: Ignore, Weight: 1/nX2
Resp. Fact. RSD: 6.462%, Coeff. Det.(r2): 0.987791
y = +0.5241x +0.0274

Anisole, 2,3,4,5,6-pentachloro-
Curve Fit: Linear, Origin: Ignore, Weight: 1/nX2
Resp. Fact. RSD: 10.66%, Coeff. Det.(r2): 0.986287
y = +0.4648x +0.0527

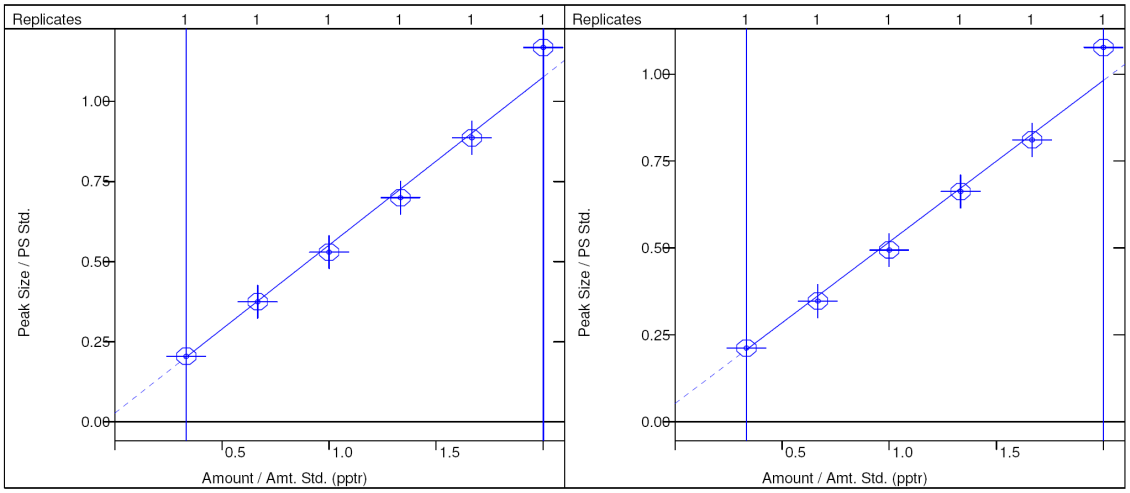

Figure 4.24: Model wine standard curve plots.

Sample Matrix	Analyte	Equation of the Line	R^2
Model Wine	TCA	y = 1.01075x + 0.196759	0.9927
	TeCA	y = 1.09192x + 0.083857	0.9868
	TBA	y = 0.52414x + 0.027367	0.9878
	PCA	y = 0.46477x + 0.052732	0.9863
David Bynum, Pinot Noir	TCA	y = 1.18464x + 0.132281	0.9906
	TeCA	y = 1.40095x + 0.059120	0.9916
	TBA	y = 0.70781x - 0.047155	0.9906
	PCA	y = 0.56191x + 0.022253	0.9921
Carlo Rossi Chardonnay	TCA	y = 1.02923x + 0.200600	0.9853
	TeCA	y = 1.36328x + 0.119982	0.9944
	TBA	y = 0.67066x + 0.044326	0.9946
	PCA	y = 0.56359x + 0.082890	0.9899

Table 4.6: Linearity data of standard addition curves.

2. Specificity

This validation parameter evaluates how efficiently the column separates the analytes from other components in the matrix. A sample of SWS#2, pinot noir, and chardonnay was spiked with 40 ng L^{-1} of each haloanisole and 30 ng L^{-1} of the internal standard 2,4,6-TCA-d_5 and was analyzed using the optimized method. The key measurements were calculated and evaluated for each analyte. A discussion of each of the measurements is given in Chapter 1.E for Equations 1.12 for R_s, 1.5 for k', 1.11 for N and N^*, and 1.13 for A_s and Chapter 3, Section D.2. The chromatogram of each matrix is included in Figure 4.25. Because the chromatograms follow the same pattern and intensities, only the pinot noir is summarized in Table 4.7.

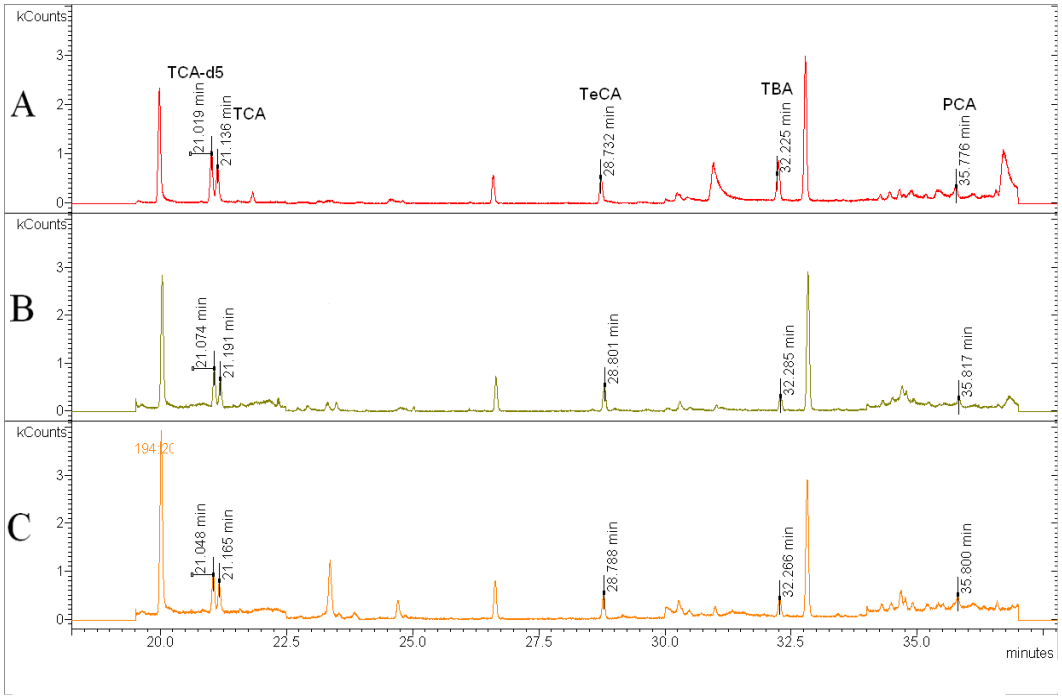

Figure 4.25: Chromatograms of spiked (A) SWS#2, (B) pinot noir, and (C) chardonnay samples.

Analyte	Resolution (R_s)	Capacity Factor (k')	Number of Theoretical Plates (N or N^*)	Peak Symmetry (A_s)
TCA-d_5	0.900	13.596	N^* = 561,883	0.913
TCA	0.900	13.678	N^* = 604,220	1.065
TeCA	18.969	18.953	N = 1,016,350	1.192
TBA	4.573	21.393	N = 1,280,153	0.966
PCA	2.272	23.837	N = 1,574,805	1.000

Table 4.7: Specificity of the pinot noir wine.

A resolution factor below 1 indicates that the adjacent peaks overlap, while R_s = 1 designates that the peaks are adequately resolved for quantitation, but do not have baseline resolution. Baseline resolution is achieved when the signal returns back to the baseline before for the start of the second peak. This

occurs when the $R_s > 1$, and is needed for good separation. For TCA-d_5 and TCA, the mass spectrometer was implemented by use of SIS to allow for quantitation of these unresolved peaks, as shown in Figure 4.23.

The capacity factor indicates the distribution of the solute between the mobile and stationary phases. A small k' indicates that the analyte interacts minimally with the stationary phase, which results in a shorter retention time. Conversely, a large k' indicates more interactions between the analytes with the stationary phase giving a longer retention time.

The effective number of theoretical plates determines how much interaction there is between the analyte and the column. The more plates there are in a given length of a column, the better separation capabilities the column will have. There are two equations used for the calculation of column efficiency. The first is labeled as *N* for peaks that exhibit a symmetrical Gaussian shape, and *N** for peaks with an asymmetrical shape.

Peak symmetry has an effect on the resolution and quantitation of analytes. A value where $A_s = 1$ indicates a symmetrical peak, where $A_s < 1$ a fronting peak and $A_s > 1$ indicates a peak which tails. In the analyzed sample none of the peaks have a mathematical symmetrical shape, but this had no effect with the quantitation.

3. Precision

Precision is often referred to as repeatability or reproducibility of the results. The precision was determined by two examinations. The first

examination calculated the relative standard deviation, *RSD*, of five SWS#2 samples with the optimized conditions and compared against the preliminary precision. This data is summarized in Table 4.8. The precision of all the haloanisoles and internal standard of the optimized method are below 2.91%.

Compound	**Model Wine Precision (n = 5) R.S.D. (%)**		
	Conc. (ng L^{-1})	**Preliminary Method**	**Optimized Method**
TCA-d_5	30	na	1.3
TCA	40	1.3	1.4
TeCA	40	4.0	1.4
TBA	40	5.5	2.3
PCA	40	6.1	2.9

Table 4.8: Method precision of preliminary and optimized methods.

The second evaluation analyzed the variation between two standard curves of the same sample matrix using the optimized method. The slopes and analyte peak area/internal standard peak area intensities were evaluated, and displayed in Figure 4.26. The slopes and intensities are predictable, except for TCA. Figure 4.27 indicates that the loss of TCA was on a linear scale. Prior to preparation of the second curve samples, the stock solution of TCA was left open in the hood vacuum. This accounted for the loss of analyte, due to TCA going into the vapor phase trying to reach an equilibrium with the headspace and sample matrix. Therefore, since the loss can be accounted for, the precision is acceptable.

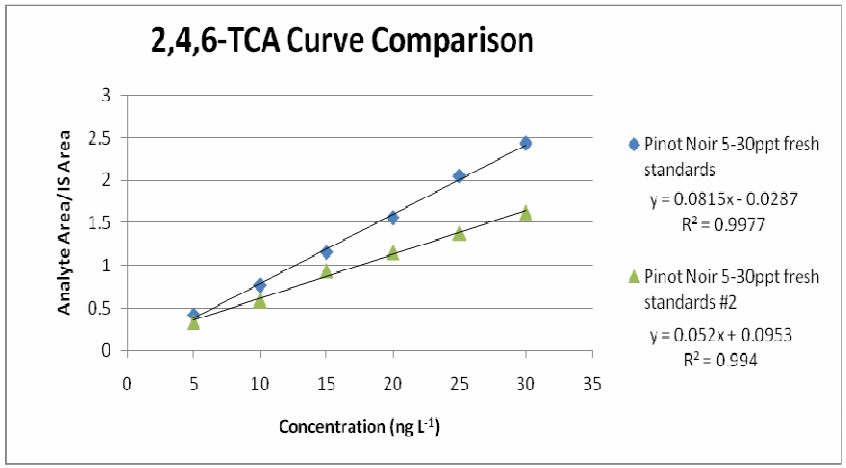

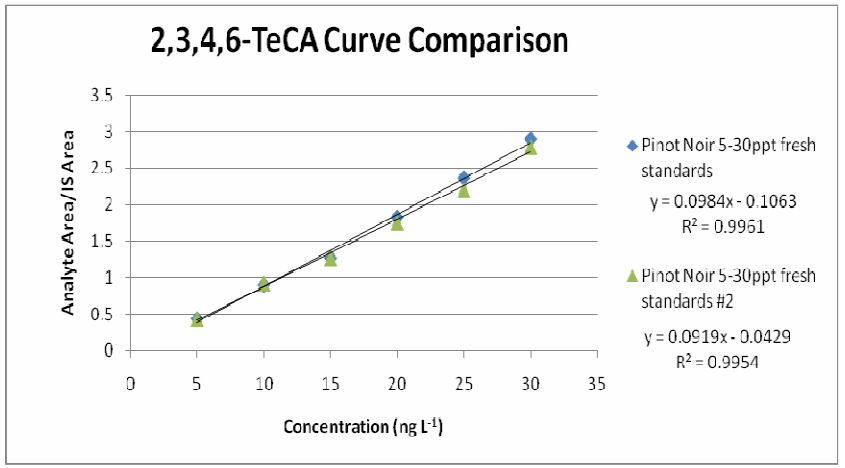

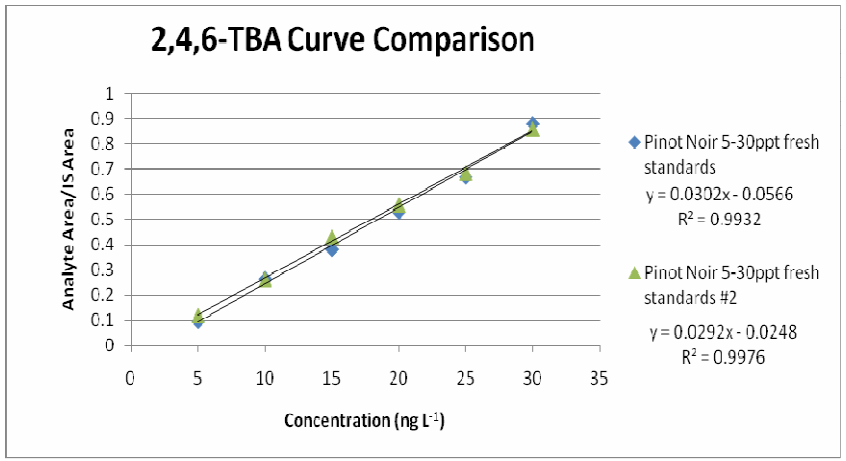

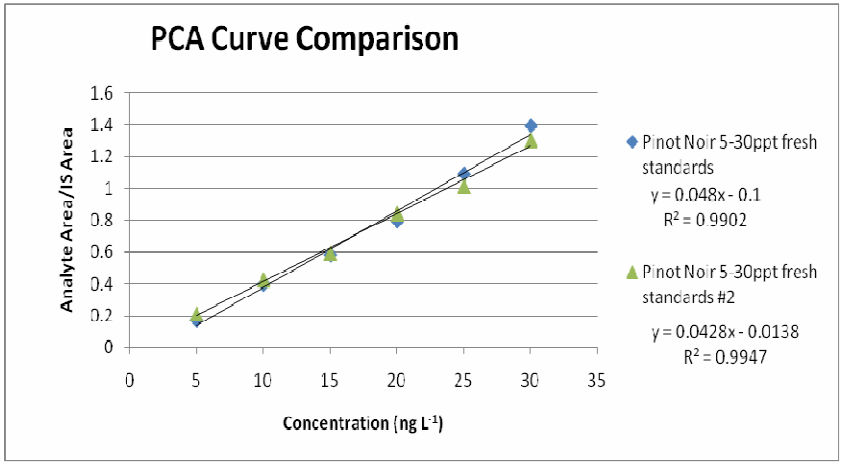

Figure 4.26: Standard addition curve reproducibility, pinot noir (5-30 ng L^{-1}).

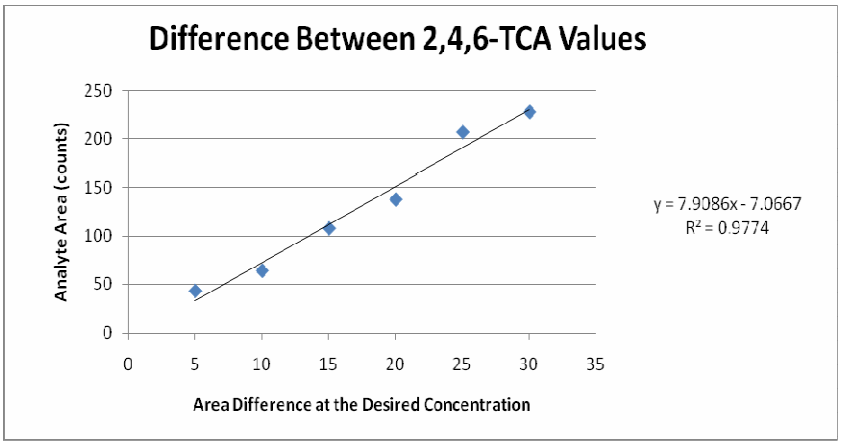

Figure 4.27: Difference between TCA standard addition curve values.

4. Sensitivity

Sensitivity is measured by an increase in the signal per unit of concentration of each individual analyte. An accurate detectable signal requires a certain amount of particles to hit the detector for the true representation of that particular analyte concentration. To test the sensitivity of the method, the scan rate was investigated to determine if there was a change in analyte response with different rates. Three SWS#2 samples were analyzed with scan rates of 0.22, 0.39, and 0.60 seconds/scan. Figure 4.28 indicates no significant difference in the scan rate versus analyte response; therefore the scan rate was not changed and kept at 0.22 seconds/scan.

Two linear standard addition curves were compared, see Figure 4.26, and the slopes and y-intercepts were evaluated. None of the y-intercepts have a value of zero, but for each curve the y-intercepts are below 0.107. As previously explained in Section F.3 of this chapter, the slopes are all acceptable, and the TCA difference can be accounted for.

Figure 4.28: Effect of scan rate on sensitivity.

Sample Matrix	Analyte	Sensitivity (counts per ng/L^{-1})
Pinot Noir	TCA	26.6
	TeCA	30.2
	TBA	8.5
	PCA	13.5

Table 4.9: Sensitivity of optimized method of Pinot Noir.

5. Limit of Detection

The limit of detection (LOD) is defined as the lowest quantity of a substance that will yield a signal at least three times that of the adjacent noise. The LOD represents the level at which the analyte is believed to be present, but not quantitatively. Table 4.10 provides a summary of the LOD of the preliminary method against the optimized method of both red and white wines. Table 4.11 compares the optimized method LOD of the red and white wines versus the olfactory thresholds. For both wines, the optimized method has a LOD which is below the olfactory perception of all haloanisoles.

Analyte	Red Wine		White Wine	
	Preliminary LOD (ng L^{-1})	Optimized LOD (ng L^{-1})	Preliminary LOD (ng L^{-1})	Optimized LOD (ng L^{-1})
TCA	3.0	1.0	3.0	2.0
TeCA	3.0	1.0	4.0	1.0
TBA	5.0	3.0	6.0	2.0
PCA	5.0	2.0	6.0	3.0

Table 4.10: Comparison of preliminary and optimized method LOD.

Analyte	Olfactory Thresholds LOD (ng L^{-1})	Red Wine LOD (ng L^{-1})	White Wine LOD (ng L^{-1})
TCA	3.0	1.0	2.0
TeCA	15.0	1.0	1.0
TBA	3.0	3.0	2.0
PCA	10000	2.0	3.0

Table 4.11: Comparison of optimized method LOD against olfactory perception [23].

6. Limit of Quantitation

The limit of quantitation (LOQ) is the lowest amount of an analyte that can be accurately and precisely measured with a signal that is of at least 10 times the adjacent noise. The purpose of at least a signal to noise (S/N) ratio of 10 is to ensure that any error, within acceptable ranges, will not have a dramatic effect on the quantitative results. Table 4.12 gives a summary of the preliminary versus the optimized LOQ of the red and white wines.

Analyte	Red Wine		White Wine	
	Preliminary LOQ (ng L^{-1})	Optimized LOQ (ng L^{-1})	Preliminary LOQ (ng L^{-1})	Optimized LOQ (ng L^{-1})
TCA	5.0	3.0	5.0	4.0
TeCA	6.0	2.0	6.0	2.0
TBA	9.0	5.0	10.0	4.0
PCA	10.0	3.0	10.0	4.0

Table 4.12: Comparison of preliminary and optimized method LOQ.

G. Analysis of Commercial Wine Samples

A new linear red wine standard addition curve was prepared with the optimized and validated method conditions. In Figure 4.29, the linear curves ranged from the limit of quantitation - 30 ng L^{-1} for the haloanisoles, and 30 ng L^{-1} for TCA-d_5. Only a red wine standard addition curve was made, because it was the only type available for the research, and is a more popular type than white wine.

Fourteen different commercial red wine samples, which were believed to be contaminated with at least one of the four haloanisoles by sensory analysis, were analyzed with the proposed optimized and validated method. The preparation of the samples is described in Chapter 2.C. Each sample was analyzed in triplicate.

A summary of the results obtained in the analysis is shown in Table 4.13. As shown in the table, every sample was contaminated with TCA, and none had a TBA contamination. TeCA and PCA were only found in two of the same samples along with TCA.

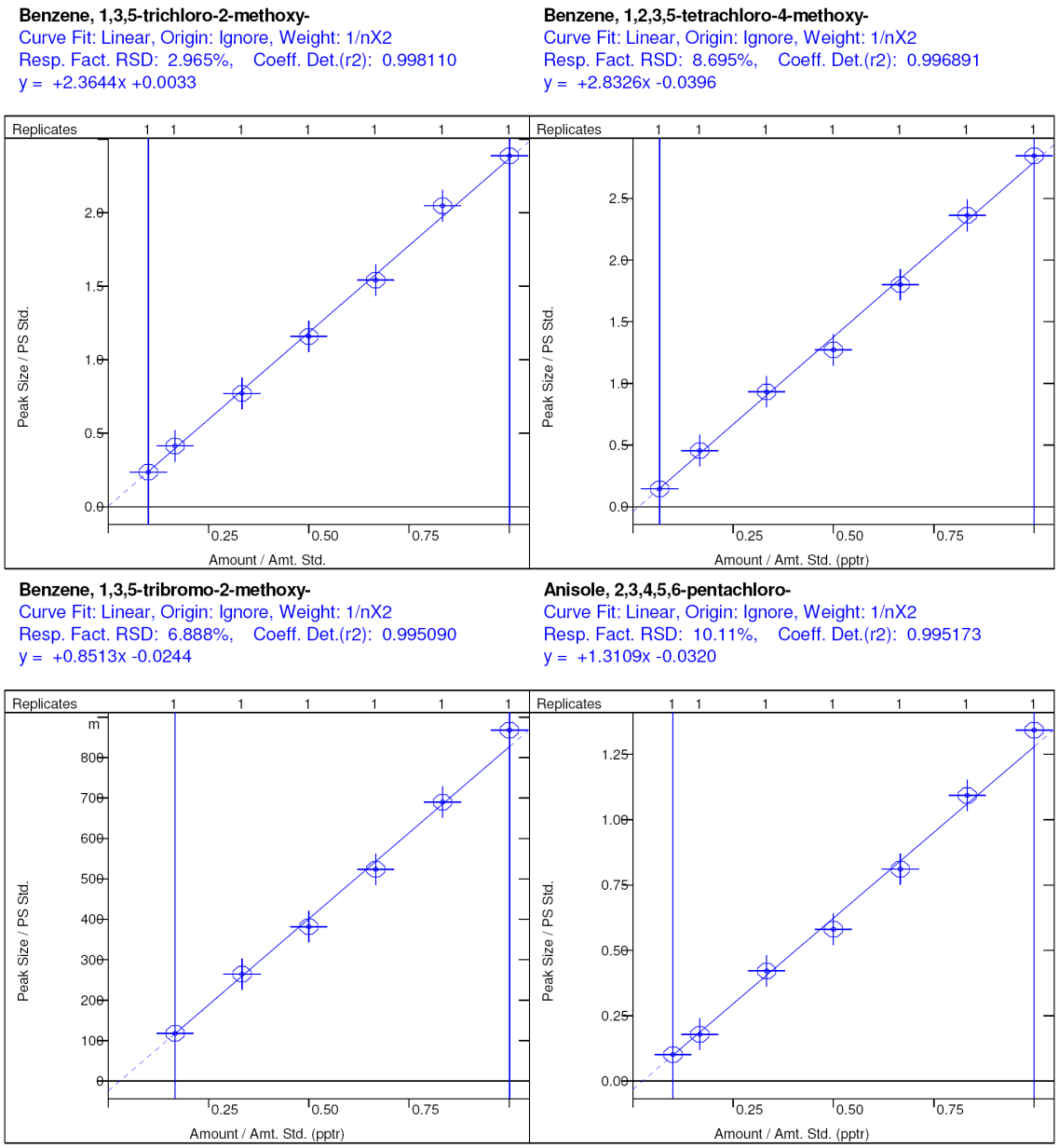

Figure 4.29: Linear standard addition curves (LOQ - 30 ng L^{-1}) used to determine the concentration of the haloanisoles present in the actual commercial samples.

Sample	Wine	Concentration ± Standard Deviation (ng L^{-1})			
		TCA	TeCA	TBA	PCA
1	2003 Turley California Zinfandel Juvenile	7.9±0.3	-	-	-
2	2000 Cuvée Réservée Chateauneaf du Pape	31.1±1.3	-	-	-
3	1999 E. Guigal Brune Et Blonde de Guigal	35.7±1.0	-	-	-
4	1993 Clos des Papes Chateauneuf du Pape	detected	17.0±0.7	-	10.8±0.6
5	2000 Chateau Chaurin Grand Cru Classé St. Emiolion	8.6±0.4	-	-	-
6	1997 McCrea Syrah	10.0±0.3	-	-	-
7	1988 Chateau Montelena Cabernet Sauvignon	20.3±0.2	detected	-	4.5±0.6
8	Las Tablas Estates Glenrose Vineyard (Syrah 35%, Mourvédre 29%, Grenache 26%, Counoise 10%)	317.1±11.8	-	-	-
9	2003 Rosenblum Cellars Zinfandel Rockpile Road Vineyard	4.0±0.2	-	-	-
10	105 Sidvri Vanderkamp Pinot Noir	19.7±0.1	-	-	-
11	Unknown #11	40.1±1.0	-	-	-
12	105 Chasseur Sexton P.N.	33.4±1.7	-	-	-
13	103 J.C. Cellars Frediani P.S.	16.6±0.1	-	-	-
14	2000 Chateau Rocher Bellevue Caprice D'Angélique	3393±54.1	-	-	-

Table 4.13: Results of the analysis of actual commercial wine samples using the optimized and validated method.

Chapter V

Conclusion

A method for the simultaneous determination of haloanisoles in wine at ultra trace amounts by solid-phase microextraction (SPME) coupled with gas chromatography-mass spectrometry (GC-MS) was developed and validated. During the optimization process, the amount of analyte transfer onto the fiber was maximized to increase overall sensitivity, limit of detection, and limit of quantitation. The two processes which had the greatest influence of the method optimization were sample preparation and the extraction procedure. The sample preparation parameters, which give the highest analyte response, were an ethanol dilution of 11% v/v with 1.0g of NaCl to 10 mL of wine (final volume). The extraction procedure that yielded the highest sensitivity of the analytes was ninety minutes at 70 °C with an injection temperature of 270 °C for seven minutes.

The proposed optimized method showed acceptable linearity for synthetic, red, and white wines. The chromatographic specificity for TeCA, TBA, and PCA were satisfactory, but TCA and TCA-d_5 needed the mass spectrometer to acquire the resolution necessary for peak integration. The precision the method shows for haloanisoles is excellent with a RSD below 2.91% for the largest value. The detection limits of the method are below the olfactory thresholds for both red and white wines and the limit of quantitation are equal to or below the odor detection threshold values.

The applicability of the optimized and validated method was demonstrated by the analysis of fourteen contaminated red wines. The results indicate that the method employed is both reliable and efficient for the determination of haloanisoles in wines at

extremely low concentrations. Therefore, this technique can be used to certify acceptance or rejection for bulk purchases of wine, and to investigate if these defects are present in wines that are not identifiable by sensory analysis.

Chapter VI

Future Work

Based upon the results of this study using solid-phase microextraction, other avenues of research have been identified and include altering fiber type, adjusting salt presence, performing multi-extractions, and undergoing multi-factorial analysis. The fiber type is a topic that may be evaluated when investigating other compounds. For haloanisoles, the literature stated the DVB/CAR/PDMS fiber gave the highest analyte sensitivity, but identified repeatability as an issue, and saturation of the fiber is difficult unless extraction is performed at high temperatures for an extremely long time (greater than 90 minutes for this study). The PA fiber is said to have better repeatability, but a lower sensitivity. Fiber type can be further evaluated for the family of compounds under analysis to determine which fiber will yield the desired results.

Sodium chloride was chosen as the noncompetitive ionic salt for "salting out" the more volatile analytes in the wine due to its availability and simple preparation. Literature states that other types or mixture of salts can be implemented and may have a greater effect to push the more volatile analytes out of solution. Na_2CO_3 makes ethanol and water immiscible, which if the desired compounds of interest are soluble in ethanol, will cause the ethanol to separate and concentrate at the top of the sample and perhaps make SPME more efficient. $(NH_4)_2SO_4$ mixed with NaH_2PO_4 [2.5:1 (w/w)] is stated to be effective at saturating the headspace during extraction more than with only sodium chloride [15]. The type of salt used may have an effect on the extraction process, and could be further investigated.

If an appropriate internal standard cannot be found, another approach used for quantitation with SPME is multiple-headspace solid-phase microextraction. This method extracts the analytes several times on the same sample until they are depleted. The concentration of the analytes decay exponentially and the total peak area related to an exhaustive extraction of the target molecules are calculated as the sum of the areas of each individual extraction. This future study can be valuable as SPME processes are regularly preformed in non-equilibrium conditions.

This research during optimization took one parameter at a time and altered it to determine the best outcome for extraction. Another approach is a full factorial design where multiple experiments are performed to determine the effects the parameters have on one another. This gives a three dimensional design where the values which yield the highest total response can be determined for the best result.

References

(1) Ribéreau-Gayon, P.; Glories, Y.; Maujean, A.; Dubourdieu, D. *The Chemistry of Wine Stabilization and Treatments*; Handbook of Enology; John Wiley & Sons, LTD: New York, NY, 2000; Vol. 2, pp

(2) Juanola, R.; Subirá D.; Salvadó, V.; Garcia, R.; Anticó E. Migration of 2,4,6-trichloroanisole from cork stoppers in wine. *Eur. Food Res. Technol.* **2005**, *220*, 347-352.

(3) Chatonnet, P.; Bonnet, S.; Boutou, S.; Labadie M.D. Identification and responsibility of 2,4,6-tribromoanisole in musty, corked odor in wine. *J. Agric. Food Chem.* **2004**, *52*, 1255-1262.

(4) Lizarraga, E.; Irigoyen, Á.; Belsue, V.; González-Peñas, E. Determination of chloroanisole compounds in red wine by headspace solid-phase microextraction and gas chromatography-mass spectrometry. *J. Chromatogr. A*. **2004**, *1052*, 145-149.

(5) Riu, M.; Mestres, M.; Busto, O.; Guasch J. Comparative study of two chromatographic methods for quantifying 2,4,6-trichloroanisole in wines. *J. Chromatogr. A*. **2007**, *1138*, 18-25.

(6) Taylor, M.K.; Young, T.M.; Butzke, C.E.; Ebeler, S.E. Supercritical Fluid Extraction of 2,4,6-Trichloroanisole from Cork Stoppers. *J. Agric. Food Chem.*, **2000**, *48*, 2208-2211.

(7) Campillo, N.; Aguinaga, N.; Viñas, P.; López-García, I.; Hernández-Córdoba, M. Purge-and-trap preconcentration system coupled to a capillary gas chromatography with atomic emission detection for 2,4,6-trichloroanisole determination in cork stoppers and wines. *J. Chromatogr. A*, **2004**, *1061*, 85-91.

(8) Soleas, G.J.; Yan, J.; Seaver, T.; Goldberg, D.M. Method for the Gas Chromatographic Assay with Mass Selective Detection of Trichloro Compounds in Corks and Wines Applied to Elucidate the Potential Cause of Cork Taint. *J. Agric. Food Chem.*, **2002**, *50*, 1032-1039.

(9) Lorenzo, C.; Zalacain, A.; Gonzalo, A.L.; Salinas, M.R. Non-destructive method to determine halophenols and haloanisoles in cork stoppers by headspace sorptive extraction. *J. Chromatogr. A*, **2006**, *1114*, 250-254.

(10) Zalacain, A.; Alonso, G.L.; Lorenzo, C.; Iñiguez, M.; Salinas, M.R. Stir bar sorptive extraction for the analysis of wine cork taint. *J. Chromatogr. A*, **2004**, *1033*, 173-178.

(11) Martínez-Uruñuela, A.; González-Sáiz, J.M.; Pizarro, C. Optimisation of a headspace solid-phase microextraction method for the direct determination of chloroanisoles related to cork taint in red wine. *J. Chromatogr. A*. **2004**, *1056*, 49-56.

(12) Vlachos, P.; Kampioti, A.; Kornaros, M.; Lyberatos, G. Matrix effect during the application of a rapid method using HS-SPME followed by GC-ECD for the analysis of the analysis of 2,4,6-TCA in wine and cork soaks. *Food Chem.* **2007**, *105*, 681-690.

(13) Pizarro, C.; Pérez-del-Notario, N.; González-Sáiz, J.M. Optimisation of a headspace solid-phase microextraction with on-fiber derivatisation method for the direct determination of haloanisoles and halophenols in wine. *J. Chromatogr. A*. **2007**, *1143*, 26-35.

(14) Martendel, E.; Budziak, D.; Debastiani, R.; Carasek, E. Determination of haloanisoles in paper samples for food packaging by solid-phase microextraction and gas chromatography. *Microchim Acta*. **2007**, *159*, 229-234.

(15) Howard, K.L. Validation of a Solid-Phase Microextraction/Gas Chromatographic Method for the Analysis of Trace Volatile Components in Chardonnay and Pinot Gris Wines. M.S. Thesis, Youngstown State University, Youngstown. OH, May 2003.

16) Martínez-Uruñuela, A.; González-Sáiz, J.M.; Pizarro, C. Multiple solid-phase microextraction in a non-equilibrium situation Application in quantitative analysis of chlorophenols and chloroanisoles related to cork taint in wine. *J. Chromatogr. A*. **2005**, *1089*, 31-38.

(17) Pizarro, C.; Pérez-del-Notario, N.; González-Sáiz, J.M. Multiple headspace solid-phase microextraction for eliminating matrix effect in the simultaneous determination of haloanisoles and volatile phenols in wines. *J. Chromatogr. A*. **2007**, *1166* , 1-8.

(18) Barker, J.; Davis, R.; Frearson, M. *Mass Spectrometry*, *Analytical Chemistry by \ Open Learning*, Second Edition; Ando, D., Ed.; John Wiley & Sons: Chichester, 1999; pp. 2.

(19) Watson, J.T. *Introduction to Mass Spectrometry*, Third Edition; Placito, M., Bialer, M., Pomes, A., Eds.; Lippincott-Raven: Philadelphia, PA, 1997; (pp2,3).

(20) http://www.microbialcellfactories.com/content/figures/1475-2859-6-6-4.jpg (accessed October 3, 2008)

(21) Jerry Pappas http://www.rci.rutgers.edu/~layla/AnalMedChem511/LCMS_files/EAS%20Ion%20Trap%20Mass%20Analyzer.pdf (accessed October 3, 2008), Quadrupole Ion-Trap Mass Analyzer, EAS Workshop.

(22) Feigal, C. Ultra Trace Analysis of Complex Matrix Samples Using Selected Ion Storage GC/MS. Varian Chromatograph Systems. Varian Application Note, Number 21.

(23) Boutou, P.; Chatonnet, P. Rapid headspace solid-phase microextraction/gas chromatographic/mass spectrometric assay for the quantitative determination of some of the main odorants causing off-flavors in wine. *J. Chromatogr. A*. **2007**, *1141*, 1-9.